

Modeling Strong and Human-Like Gameplay with KL-Regularized Search

Athul Paul Jacob^{*12} David J. Wu^{*1} Gabriele Farina^{*3} Adam Lerer¹ Anton Bakhtin¹ Jacob Andreas²
Noam Brown¹

Abstract

We consider the task of building strong but human-like policies in multi-agent decision-making problems, given examples of human behavior. Imitation learning is effective at predicting human actions but may not match the strength of expert humans, while self-play learning and search techniques (e.g. AlphaZero) lead to strong performance but may produce policies that are difficult for humans to understand and coordinate with. We show in chess and Go that regularizing search policies based on the KL divergence from an imitation-learned policy by applying Monte Carlo tree search produces policies that have higher human prediction accuracy and are stronger than the imitation policy. We then introduce a novel regret minimization algorithm that is regularized based on the KL divergence from an imitation-learned policy, and show that applying this algorithm to no-press Diplomacy yields a policy that maintains the same human prediction accuracy as imitation learning while being substantially stronger.

1. Introduction

Self-play AI algorithms have matched or exceeded expert human performance in many games, such as chess (Campbell et al., 2002; Silver et al., 2018), Go (Silver et al., 2016; 2017), and poker (Moravčík et al., 2017; Brown & Sandholm, 2017; 2019). However, the resulting policies often differ markedly from how humans play (McIlroy-Young et al., 2020a). This is a serious problem for human-computer interactions that involve cooperation rather than purely competition. In such settings, modeling the other participants accurately is important for success. For example, it is important for a self-driving car at a four-way stop sign to conform to existing human conventions rather than its own self-play solution to the problem (Lerer & Peysakhovich,

2019). Moreover, even in purely adversarial games, the alien nature of AI policies makes it difficult for humans to understand and learn from superhuman bots.

The straightforward path toward modeling human behavior in multi-agent interactions is imitation learning on human data. However, evidence in multiple games indicates that while imitation learning on expert human data outperforms other methods at predicting human actions, in domains with complex strategic planning it produces policies that are much weaker than actual expert human play. There therefore appears to be a binary choice between using self play to generate strong but inhuman policies, or using imitation learning to generate human-like but weak policies.

In this paper, we study the problem of producing policies that are simultaneously *strong* and *human-like* in games with complex strategic planning like chess, Go and Diplomacy. In all three, we find that conducting search with KL-regularization towards an imitation-learned policy significantly improves upon the prior state-of-the-art on this problem. In fact, rather than merely interpolating between the advantages of unregularized search and pure imitation learning, we show that KL-regularized search largely obtains the benefits of both and sometimes even exceeds the accuracy of pure imitation learning or the strength of unregularized search.

In Section 3, we show that Monte Carlo tree search (MCTS) with a human imitation-learned policy prior and value function surpasses prior state-of-the-art results for human prediction accuracy in chess and Go. As explained by Grill et al. (2020), standard MCTS with a policy prior can be viewed as a form of KL-regularized search, optimizing a value function subject to a KL-divergence term with that prior. Although MCTS has been extensively studied for developing strong agents, it has been explored much less in the context of developing human-like agents, and we show with a human-learned prior it is highly effective at the latter.

Section 4 builds on these findings and shows how to generalize them to a class of imperfect-information games (in which ordinary MCTS is unsound and cannot be applied) via a new algorithm for KL-regularized regret minimization. While search via regret minimization has achieved superhuman performance in purely adversarial imperfect-

^{*}Equal Contribution. ¹Meta AI Research, New York, NY, USA
²CSAIL, MIT, Cambridge, MA, USA ³School of Computer Science, Carnegie Mellon University, Pittsburgh, PA, USA. Correspondence to: Athul Paul Jacob <apjacob@mit.edu>, David J. Wu <dwu@fb.com>, Gabriele Farina <gfarina@cs.cmu.edu>, Noam Brown <noambrown@fb.com>.

information games like poker and two-player Diplomacy, recent results suggest that in 7-player no-press Diplomacy it arrives at a policy that is incompatible with typical human play (Bakhtin et al., 2021). We show that existing unregularized regret minimization algorithms achieve low accuracy in predicting expert human actions in Diplomacy. We then introduce the first regret minimization algorithm to incorporate a cost term proportional to the KL divergence between the search policy and a human-imitation learned **anchor policy**. We call this algorithm **policy-regularized hedge**, or **piKL-hedge**. We prove that piKL-hedge converges to an equilibrium in which all players’ policies are optimal given the joint policies of the players and the cost of deviating from the anchor policy. We then present experimental results in no-press Diplomacy showing that piKL-hedge can produce policies that predict human actions as accurately as imitation learning while also improving head-to-head performance in a population of prior agents.

Our experiments demonstrate the benefits of KL-regularized search in all three of chess, Go, and no-press Diplomacy to producing agents that are simultaneously more human-like and closer in strength to actual human experts than purely imitation-learned models.

2. Preliminaries

We study the problem of learning policies for multiplayer games. Here we briefly introduce the key ingredients of both classes of games we study; Section 3 and Section 4 give a more formal presentation tailored to individual game types and learning algorithms.

An (N -player) game is defined by a **state space** S , an **action space** A , a (deterministic) **transition function** $T : S \times A^N \rightarrow S$, and a collection of **reward functions** u_i . We model the behavior of each player in a game as a **policy** $\pi_i : S \rightarrow \Delta(A)$ (a distribution over actions given states). In every round of a game, each player observes a (possibly incomplete) view s_i^t of the current state. One or more players select actions $a_i^t \sim \pi_i(\cdot \mid s_i^t)$ after which each player receives a reward $u_i^t(s^t, \mathbf{a}^t = a_1^t, \dots, a_n^t)$, and the game transitions into a new state $s^{t+1} = T(s^t, \mathbf{a}^t)$. An **optimal policy** is one that maximizes the agent’s expected reward. The set of optimal policies for agent i depends on the policies $\pi_{-i} = \{\pi_1, \dots, \pi_{i-1}, \pi_{i+1}, \dots, \pi_N\}$ for the other players.

The sequential decision-making problem described above is extremely general, and in this paper we focus on two special cases. In **perfect-information** games, players make moves sequentially (e.g., u^1 and s^2 depend only on a_1 , u^2 and s^3 depend only on a^2 , etc.). Many important games, including chess and Go, fall into this category. Next, we study a more general class of **imperfect-information, simultaneous-**

action games that make no assumptions about the dependence of different u_i and T on \mathbf{a} ; here we focus on games with only a single round, also called matrix games.

Owing to the large differences between these two settings, the definitions of policy optimality and the tools for computing optimal policies are quite different. The remainder of this paper accordingly offers a deeper exploration of each class of games: perfect-information games in Section 3 and imperfect-information games in Section 4, with a more detailed formal treatment of each class of games in the corresponding section.

3. Perfect-Information Games: Policy Regularization in Monte Carlo Tree Search

In this section, we focus on developing strong human-like agents for perfect-information games. Monte Carlo tree search (MCTS) has been highly successful for developing strong, but not necessarily human-like agents in this setting, and is a key component of general learning algorithms such as AlphaZero and MuZero capable of achieving superhuman performance in chess, Go, and similar games (Silver et al., 2018; Schrittwieser et al., 2020). By contrast, for developing human-like agents, the best prior human move prediction accuracies for chess and Go were all achieved with pure supervised models on human data (McIlroy-Young et al., 2020a; Cazenave, 2017; Silver et al., 2017).

The state of the art for predicting human moves in chess is the Maia engine created by McIlroy-Young et al. (2020a) via pure imitation learning without any search. However, this approach appears to be of limited effectiveness for modeling sufficiently strong humans. Although the weakest Maia models at low temperatures appear to outperform the players they imitate (due to “averaging away” of the imitated players’ individual idiosyncratic mistakes (Anderson et al., 2021)) each successive model on data from stronger players improves by much less than the players improve.¹ The strongest model, trained to predict human 1900-1999 rated players, even with low temperature appears to be clearly below a 1950-average level of performance in all but the minority of bullet-speed games (in which very little time is available for planning and players are forced to rely more heavily on intuition).

Similarly, in Go, pure imitation-learning agents typically have not exceeded mid-expert level on various online servers despite being trained on top-expert games (Cazenave, 2017). Although the models may achieve reasonable per-move prediction accuracy or cross-entropy, they clearly fail to capture important dimensions of human play, as evidenced by their

¹See ratings data at <https://lichess.org/@/maia1>, <https://lichess.org/@/maia5>, <https://lichess.org/@/maia9>

lack of competitiveness over the whole game.²

In contrast, search-based RL agents such as AlphaZero that do not make use of a human policy prior play at a superhuman level, but often play in non-human ways that humans find difficult to understand even when given direct access to interactively query and inspect the agent’s analysis (Silver et al., 2017; Egri-Nagy & Törmänen, 2020).

However, we show in both chess and Go that if the human-learned model is used in MCTS with appropriate parameters, MCTS outperforms those models’ human prediction accuracy while simultaneously reducing the shortcomings in those models’ strength.

3.1. Background

We consider sequential games where each player i alternatively chooses action a from a policy π_i where, $a \sim \pi_i(\cdot | s)$. Each action deterministically transitions the game into a new state $s' = T(s, a)$ and gives rewards $u_i(s, a)$. Notationally, we may elide the player i in some places when it is clear that i is the next player to move in the state being considered.

For this work, following Silver et al. (2016), we implement one of the most common modern forms of MCTS, which uses a value function V predicting the expected total future reward $V_i(s) = \mathbb{E}[\sum_t u_i(s_t, a_t) | \pi_1, \pi_2, s_0 = s]$ and a policy prior τ (typically both the outputs of a trained deep neural net) and attempts to produce an improved policy π .

Each turn, MCTS builds and expands a game tree over multiple iterations rooted at the current state for that turn. On each iteration t MCTS starts at the root and descends the tree by exploring at each state s an action a according to some exploration method. Upon reaching a state s_t not yet explored, it adds s_t to the tree, queries the value function $V_i(s_t)$ for each i , and updates the statistics of all nodes traversed based on $V_i(s_t)$ and any intermediate rewards received. Subsequent iterations begin again from the root.

The statistics tracked at the node for each state s where player i is to move include the visit counts $N(s, a)$ which are the number of iterations that reached state s and tried action a , and $Q(s, a)$ the average value of those iterations, i.e. $Q(s, a) = (1/N(s, a)) \sum_t V_i(s_t) + U_i(s, s_t)$ where the sum ranges only over those iterations t that reached state s and tried action a and $U_i(s, s_t)$ is the total intermediate reward on the path from s to s_t . When descending the tree, the exploration method is to always select the action:

$$\arg \max_a Q(s, a) + c_{\text{puct}} \tau(s, a) \frac{\sqrt{\sum_b N(s, b)}}{N(s, a) + 1} \quad (1)$$

² Anecdotal observation among Go players suggests that these models may play well for a while, but uncharacteristically blunder in ways well below their equivalent human level in tactics.

where $\tau(s, a)$ is the prior policy probability for action a in state s , and c_{puct} is a tunable parameter controlling the tradeoff between exploration and exploitation. See also Appendix I for a subtle algorithmic detail. The final agent policy π is simply proportional to the visit counts for the root, i.e. $\pi(s, a) = N(s, a) / \sum_b N(s, b)$ where s is the root state, or optionally we may also have $\pi(s, a) \sim N(s, a)^{1/T}$ where T is a temperature parameter.

Grill et al. (2020) show that the final agent policy π computed by this form of MCTS is an approximate solution to the optimization problem:

$$\arg \max_{\pi} \sum_a Q(s, a) \pi(s, a) + \lambda D_{\text{KL}}(\tau \| \pi) \quad (2)$$

where $\lambda \sim c_{\text{puct}} \sqrt{N}$ and N is the total number of iterations performed.

In other words, at every node of the tree simultaneously, MCTS implicitly optimizes its expected future reward subject to KL regularization of its policy towards the prior policy τ with strength controlled by λ . For any fixed computational budget N , we can therefore tune c_{puct} to vary the strength of that prior, with $c_{\text{puct}} = \infty$ approximating the prior policy before search, and $c_{\text{puct}} = 0$ approximating a greedy argmax according to the running Q value estimates, and we test a range of values in our experiments. See Grill et al. (2020) for more quantitative bounds on the quality and convergence of this approximation.

If our goal is a strong *human-like* agent rather than solely a strong agent, and the KL-regularizing policy is learned from human data, then that policy serves not just as a prior, but also as an **anchor policy** that regularizing towards is desirable in and of itself. MCTS provides a possibility to improve that policy while remaining close to human. Our experiments confirm that MCTS improves on the strength and human prediction accuracy of the best existing models in both chess and Go.

3.2. Experiments in Chess and Go

In chess and Go, we ran two main experiments each. First, in chess using the prior state-of-the-art Maia models from McIlroy-Young et al. (2020a) and in Go using a model trained on professional games from the GoGoD dataset, we demonstrate that MCTS with that model outperforms the raw model in human prediction accuracy. Second, we also sanity-check that MCTS with the same parameters greatly improves the strength of the same models in chess and Go.

3.2.1. DATA AND MODEL ARCHITECTURE

In chess, for the human-learned anchor policy we use the pre-trained Maia1100, Maia1500, and Maia1900 models from McIlroy-Young et al. (2020a), achieving state-of-the-

| Model | Predicting | (raw model) | $c_{\text{puct}} = 10$ | $c_{\text{puct}} = 5$ | $c_{\text{puct}} = 2$ | $c_{\text{puct}} = 1$ | $c_{\text{puct}} = 0.5$ |
|---------------|------------|-------------|------------------------|-----------------------|-----------------------|-----------------------|-------------------------|
| Maia1100+MCTS | 1100 | 51.2 | 51.3 | 51.4 | 50.9 | 49.6 | 47.5 |
| Maia1500+MCTS | 1500 | 52.6 | 52.8 | 53.0 | 52.9 | 52.0 | 50.0 |
| Maia1900+MCTS | 1900 | 53.2 | 53.6 | 54.0 | 54.4 | 53.8 | 52.4 |

Table 1. Maia top-1 % test accuracy predicting human chess players in rating buckets 1100, 1500, 1900 using MCTS with 50 playouts and various c_{puct} , or raw model without MCTS. Approx 10k games per bucket, first 11 ply of each game and moves with < 30s time left excluded, similar to (McIlroy-Young et al., 2020a). Standard error is approximately 0.1 or less on all values. MCTS improves human prediction accuracy for all players, more for higher-rated players.

| Cazenave (2017) | Wu (2018) | Ours (raw model) | Ours + MCTS | | | | |
|-----------------|-----------|------------------|------------------------|-----------------------|-----------------------|-----------------------|-------------------------|
| | | | $c_{\text{puct}} = 10$ | $c_{\text{puct}} = 5$ | $c_{\text{puct}} = 2$ | $c_{\text{puct}} = 1$ | $c_{\text{puct}} = 0.5$ |
| 54.7 | 55.3 | 57.8 | 58.1 | 58.3 | 58.5 | 58.1 | 57.1 |

Table 2. Top-1 % test accuracy predicting professional moves in Go on the GoGoD dataset using MCTS with 50 playouts and various c_{puct} , or raw model without MCTS. Standard error is approximately 0.1 or less on all values. Our model predicts top human player moves more accurately than prior models, MCTS improves accuracy even further.

art performance on rating-conditional human move prediction in chess,. These models follow a standard AlphaZero-like residual block architecture, including both a policy and a value head, and were trained to imitate players in ratings “buckets” 1100, 1500, and 1900 respectively, based on roughly 10 million games each from the popular Lichess server (each bucket contains games between players from rating N to $N+99$). For Go, we trained a deep neural net

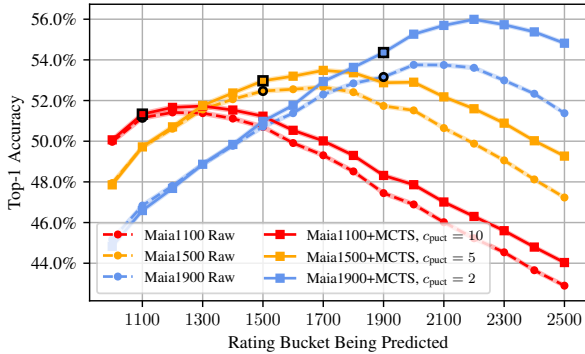


Figure 1. Top-1 % test accuracy in chess for Maia models trained to predict moves by players in rating buckets 1100, 1500, 1900, applied to predict all *other* rating buckets, without and with MCTS, and with a reasonable c_{puct} for each model. The black bolded outline indicates where the model is predicting the same rating as it was trained on. Standard error is very small, equal to the slight shaded thickness around each line. MCTS most improves prediction of a model on players of its target rating and higher.

on the GoGoD professional game dataset³. We match the practice of Cazenave (2017) in using games from 1900 through 2014 for training and 2015-2016 as the test set, with roughly 73000 and 6500 games, respectively. Our ar-

³<https://gogodonline.co.uk/>

chitecture matches the 20-block residual net structure used by some versions of AlphaZero (Silver et al., 2017), except adds squeeze-and-excitation layers which have been successful in image processing tasks (Hu et al., 2018), and are now common in self-play learning in chess and Go (LC0, 2020; Troisi, 2019). See Appendix H for additional details.

3.2.2. IMPROVED HUMAN PREDICTION

In Table 1 we show the top-1 accuracy of Maia with MCTS at predicting players of various ratings. MCTS on top of each model outperforms that model at predicting human moves. The benefit provided increases greatly as the level of players predicted increases, which is consistent with the intuitive hypothesis that stronger players plan more deeply, increasing the value of explicitly modeling that planning.

The optimal parameter choice for c_{puct} appears to decrease as the rating of the players being predicted increases. Smaller c_{puct} allows greater deviation from the prior policy based on smaller Q-value differences from search. This accords well with the intuitive notion that stronger players are more sensitive to small future value differences when they plan ahead.

In Figure 1, we see that while KL-regularized search improves each model’s accuracy on players of its target rating, surprisingly, the improvement grows yet larger when each model predicts players of *higher* rating than it was trained on. This suggests that as human players improve, the incremental average change in their behavior resembles or is correlated with the way that highly-regularized search improves the strength of a baseline policy.

In Table 2 we show similar accuracy improvements for Go. Search outperforms the raw model at the very same

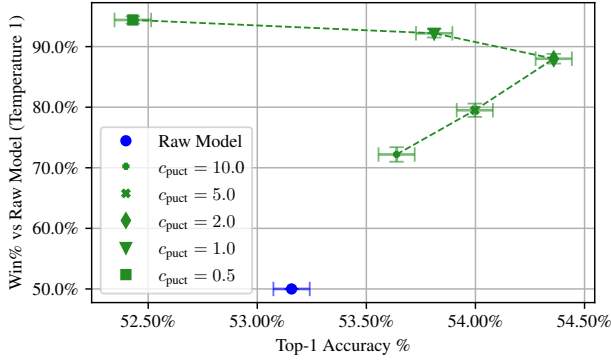


Figure 2. Maia1900 top-1 accuracy predicting human chess players in rating bucket 1900 with and without MCTS from Table 1, plotted versus temperature 1 winrates from Table 3, error bars indicate 1 standard error. Many c_{puct} values increase both human prediction accuracy and winrate over the raw model.

task of predicting humans that the model was trained to accomplish. Our top accuracy for the GoGoD professional games dataset, 58.5%, is to our knowledge the highest test accuracy achieved on this dataset by any means.

Lastly, in Appendix C, we show that if we apply post-processing based on Grill et al. (2020) that directly solves the KL-regularized optimization problem that MCTS is a discrete approximation of, MCTS improves cross entropy with human moves in both chess and Go, not just top-1 accuracy. In other words, not only does policy-regularized search improve the prediction of the top move, but it also better models the overall *distribution* of moves that humans may likely play.

| Game | c_{puct} | MCTS Win% vs raw model | |
|-------|-------------------|------------------------|------------------|
| | | temp = 1 | temp = 0.3 |
| Chess | 10.0 | 72.2% \pm 1.2% | 62.4% \pm 1.3% |
| Chess | 5.0 | 79.5% \pm 1.1% | 72.3% \pm 1.2% |
| Chess | 2.0 | 88.0% \pm 0.8% | 86.1% \pm 0.9% |
| Chess | 1.0 | 92.2% \pm 0.7% | 92.9% \pm 0.6% |
| Chess | 0.5 | 94.4% \pm 0.6% | 94.7% \pm 0.5% |
| Go | 10.0 | 73.2% \pm 1.4% | 63.3% \pm 1.5% |
| Go | 5.0 | 80.5% \pm 1.3% | 74.1% \pm 1.4% |
| Go | 2.0 | 87.6% \pm 1.0% | 85.3% \pm 1.1% |
| Go | 1.0 | 94.6% \pm 0.7% | 94.4% \pm 0.7% |
| Go | 0.5 | 96.4% \pm 0.6% | 97.0% \pm 0.5% |

Table 3. Winrate of base model + MCTS vs base model at temperature 1 and 0.3. Base model is Maia1900 in chess, and our GoGoD model in Go. 1000 games per figure, draws count as half a win, \pm indicates one standard error. Go uses Japanese rules with 6.5 komi. MCTS greatly improves strength in Chess and Go, the smallest c_{puct} values improve it most.

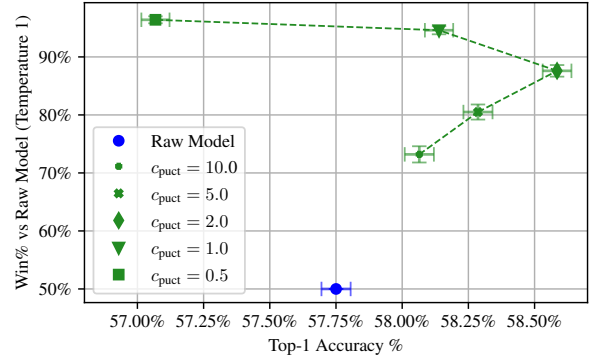


Figure 3. Top-1 accuracy predicting human Go players in GoGoD dataset with and without MCTS from Table 2, plotted versus temperature 1 winrates from Table 3, error bars indicate 1 standard error. Many c_{puct} values increase both human prediction accuracy and winrate over the raw model.

3.2.3. IMPROVED PLAYING STRENGTH

As discussed earlier, there is a significant gap of 100 to 300 Elo in Maia1900’s performance at all but bullet time controls against the players it attempts to imitate. The same is observed in Go with the best imitation-learning models only reaching mid-expert level even when trained on top-expert and professional games.⁴

In both chess and Go, we sanity-check that MCTS does provide a large strength improvement. We play 1000 games between the raw model sampling moves at temperature 1 or 0.3 and an MCTS agent sampling moves via the root visit counts with the same temperature with each setting. In Go, we also use the open-source KataGo (Wu, 2020) to determine when the game is over and to score the result.⁵

Table 3 confirms in both chess and Go that MCTS does provide large improvements in strength. Notably, playing strength is maximized at low values of $c_{\text{puct}} = 0.5$ or possibly even smaller, below the range of values that perform well at human prediction. This shows the importance of adjusting this parameter, and possibly one factor in why it may have remained relatively unnoticed that MCTS can greatly improve human prediction – engines that have already optimized their parameters for strength, even when using a human model as a prior, will likely not be using parameters ideal for matching human behavior.

However, even within the same range of parameters that

⁴Pure imitation-learning agents have historically achieved ratings from 1 dan to 5 dan on online servers, but rarely ever higher.

⁵Unlike RL agents, humans which our models imitate universally pass and score the game well before it becomes mechanically scorable. We therefore use KataGo as a neutral judge of when players would pass and to score the result.

improve human prediction accuracy, MCTS still provides large strength gains. Figures 2 and 3 show the relationship between these results. Although we did not test against humans directly to calibrate strength gains, our results provide clear evidence that a well-tuned human-regularized MCTS agent would be far closer in overall strength level to the 1900-1999-rated players that Maia1900 currently falls short of imitating, while simultaneously being more accurate to their behavior on a move-by-move basis. Our results provide clear evidence for this in Go as well.

4. Imperfect-Information Games: Policy-regularized Regret Minimization

While MCTS is a popular search algorithm for perfect-information deterministic games, it is not able to compute optimal policies in imperfect-information games. Instead, iterative algorithms based on regret minimization are the leading approach to search in imperfect-information games.

Hedge (Littlestone & Warmuth, 1994; Freund & Schapire, 1997) is an iterative regret minimization algorithm that in general converges to a coarse correlated equilibrium (CCE) (Hannan, 1957). In the special case of two-player zero-sum games, it also converges to a Nash equilibrium (NE) (Nash, 1951).

Regret Matching (RM) (Blackwell et al., 1956; Hart & Mas-Colell, 2000) is another equilibrium-finding algorithm similar to Hedge that has historically been more popular and that we compare our algorithm to in this paper.

The effectiveness of the implicit KL-regularization in MCTS that we study in Section 3 motivates us to develop an equilibrium-finding algorithm called piKL-Hedge that similarly biases the search towards an anchor policy. In Section 4.3, we show empirically that piKL-Hedge achieves better performance against baseline human-imitation models than Hedge and Regret Matching in a large imperfect-information game, as well as much higher human prediction accuracy.

4.1. Background

We consider a game with \mathcal{N} players where each player i chooses an action a from a set of actions \mathcal{A}_i . We denote the actions of all players other than i as \mathbf{a}_{-i} . After all players simultaneously choose an action, player i receives a reward of $u_i(a, \mathbf{a}_{-i})$. Players may also choose a probability distribution over actions, where the probability of action a is denoted $\pi_i(a)$ and the vector of probabilities is denoted π_i . We also define the fixed policy that we are interested in biasing player i towards as the anchor policy $\tau_i \in \Delta(\mathcal{A}_i)$.

Each player i maintains a **regret** value for each action. The regret on iteration t is denoted $R_i^t(a)$. Initially, all regrets are

zero. On each iteration t of Hedge, $\pi_i^t(a)$ is set according to

$$\pi_i^t(a) \propto \exp(R_i^t(a)) \quad (3)$$

Next, each player samples an action a^* from \mathcal{A}_i according to π_i^t and all regrets are updated such that

$$R_i^{t+1}(a) = R_i^t(a) + u_i(a, \mathbf{a}_{-i}^*) - \sum_{a' \in \mathcal{A}_i} \pi_i^t(a') u_i(a', \mathbf{a}_{-i}^*) \quad (4)$$

It is proven that the *average* policy of Hedge over all iterations converges to a NE in two-player zero-sum games and, more broadly, the players' joint policy distribution converges to a CCE as $t \rightarrow \infty$.

We wish to model agents that seek to maximize their expected reward in the game, while at the same time playing “close” to the anchor policy. The two goals can be reconciled by defining a composite utility function that adds a penalty term based on the “distance” between the player policy and their anchor policy, with coefficient $\lambda_i \in [0, \infty)$ scaling the penalty.

For each player i , we define i 's utility as a function of the the agent policy $\pi_i \in \Delta(\mathcal{A}_i)$ given policies π_{-i} of all other agents:

$$\mathcal{U}_i(\pi_i, \pi_{-i}) := u_i(\pi_i, \pi_{-i}) - \lambda_i D_{\text{KL}}(\pi_i \parallel \tau_i). \quad (5)$$

When λ is large, the utility function is dominated by the KL-divergence term $\lambda_i D_{\text{KL}}(\pi_i \parallel \tau_i)$, and so the agent will naturally tend to play a policy π_i close to the anchor policy τ_i . When λ_i is small, the dominating term is the rewards $u_i(\pi_i, \mathbf{a}_{-i}^*)$ and so the agent will tend to maximize reward without as closely matching the anchor policy τ_i . These statements are made precise in Theorem 1 and Theorem 2.

The careful reader may observe that the direction of the KL-divergence term, $D_{\text{KL}}(\pi \parallel \tau)$ is the opposite of the direction implicit in MCTS, $D_{\text{KL}}(\tau \parallel \pi)$. We choose this direction for greater ease of theoretical analysis and implementation in the context of regret minimization; for our use cases we have not found the exact form of the loss to be critical so much as simply doing any reasonable regularized search.

4.2. No-Regret Learning for Policy-Regularized Utilities

In this section, we present a no-regret algorithm based on Hedge for any player i to learn strong policies relative to the regularized utilities defined in (5). More specifically, we present Algorithm 1 and show it guarantees that each player i accumulates sublinear regret with respect to the utility functions:

$$\mathcal{U}_i^t(\pi_i) := \mathcal{U}_i(\pi_i, \mathbf{a}_{-i}^t) = u_i(\pi_i, \mathbf{a}_{-i}^t) - \lambda_i D_{\text{KL}}(\pi_i \parallel \tau_i),$$

no matter the opponents' actions \mathbf{a}_{-i}^t at each time t .

In the next corollary of Proposition 1 we show that the distance of $\bar{\pi}_i^T$ from the anchor policy τ_i in the limit grows inversely proportional to the parameter λ_i .

Algorithm 1 piKL-HEDGE (for Player i)

Data: • A_i set of actions for Player i ;
 • u_i reward function for Player i ;
 • $\eta > 0$ learning rate hyperparameter.

```

1 function INITIALIZE()
2    $t \leftarrow 0$ 
3   for each action  $a \in A_i$  do
4      $CV_i^0(a) \leftarrow 0$ 
5 function PLAY()
6    $t \leftarrow t + 1$ 
7   let  $\pi_i^t$  be the policy such that
8
9     
$$\pi_i^t(a) \propto \exp \left\{ \frac{\eta CV_i^{t-1}(a) + t\lambda_i \eta \log \tau_i(a)}{1 + t\lambda_i \eta} \right\}. \quad (6)$$

10  sample an action  $a^t \sim \pi_i^t$ 
11  play  $a^t$  and observe actions  $\mathbf{a}_{-i}^t$  played by the opponents
12  for each  $a \in A_i$  do
13     $CV_i^t(a) \leftarrow CV_i^{t-1}(a) + u_i(a, \mathbf{a}_{-i}^t)$ 
    
```

Proposition 1. Fix a player $i \in \{1, \dots, n\}$. The regret

$$R_i^T := \max_{\pi^* \in \Delta(A_i)} \sum_{t=1}^T \mathcal{U}_i^t(\pi^*) - \sum_{t=1}^T \mathcal{U}_i^t(\pi_i^t)$$

incurred up to any time T by policies π_i^t defined in (6) where the learning rate is set to any value $0 < \eta \leq 1/(\lambda_i \beta_i + 2D_i)$, satisfies

$$R_i^T \leq \frac{\log |A_i|}{\eta} + \frac{3e(1 + \log T)}{\lambda_i \eta} (D_i + \lambda_i \beta_i + \lambda_i \sqrt{|A_i|}),$$

where D_i is any upper bound on the range of the possible rewards of Player i , and

$$\beta_i := \max_{a \in A_i} \log(1/\tau(a)). \quad (7)$$

Proposition 1 immediately implies that the average regret accumulated by each player grows at a sublinear rate of roughly as $O(\log(T)/T)$.

As with many other regret-minimization methods, we consider the *average* policy of each player i over T iterations:

$$\bar{\pi}_i^T := \frac{1}{T} \sum_{t=1}^T \pi_i^t \quad (8)$$

where π_i^t is defined in (6). We take $\bar{\pi}_i^T$ to be the final agent policy produced by piKL-HedgeBot. From Proposition 1,

we can immediately derive the following theorem that the KL-divergence of $\bar{\pi}_i^T$ from the anchor policy τ_i converges to be inversely proportional to the parameter λ_i .

Theorem 1. (*piKL stays close to the anchor policy*) Upon running Algorithm 1 for any T iterations in any multiplayer general-sum game, the average policy $\bar{\pi}_i^T$ of any player i is at a distance

$$D_{\text{KL}}(\bar{\pi}_i^T \parallel \tau_i) \leq \frac{1}{\lambda_i} \left(\frac{R_i^T}{T} + D_i \right).$$

In particular, if $\eta > 0$ is set so that $R_i^T = o(T)$, then $D_{\text{KL}}(\bar{\pi}_i^T \parallel \tau_i) \rightarrow D_i/\lambda_i$ as $T \rightarrow \infty$.

We can also show in the case of a two-player zero-sum game that $\bar{\pi}_i^T$ approximates a Nash equilibrium of the original utility functions, similarly controllable by λ :

Theorem 2. Let $(\bar{\pi}_1, \bar{\pi}_2)$ be any limit point of the average policies $(\bar{\pi}_1^T, \bar{\pi}_2^T)$ of the players. Almost surely, $(\bar{\pi}_1, \bar{\pi}_2)$ is a $(\max_{i=1,2} \{\lambda_i \beta_i\})$ -approximate Nash equilibrium policy with respect to the original utility functions u_i , where β_i is as defined in (7).

For detailed proofs, see Appendix A.

Lastly, we remark that in the special case that τ_i is the uniform policy for all players i , the above results imply that Algorithm 1 converges towards a **quantal response equilibrium** (McKelvey & Palfrey, 1995a), in which an imperfect agent is modeled as choosing actions with probability exponentially decaying in the amount that each action is worse than the best action(s), given that all other agents behave the same way. Our method can be seen as a generalization that takes into account a human-learned prior for what actions may be more likely.

4.3. Experiments in Diplomacy

Diplomacy's 7-player simultaneous-action and mixed competitive and cooperative incentives, as well as its large combinatorial action space, make tree-search methods like MCTS infeasible. Instead, the prior leading approaches to conducting search in Diplomacy have applied 1-ply regret matching (Gray et al., 2020; Bakhtin et al., 2021). However, unlike in two-player zero-sum games, due to Diplomacy's mixed cooperative/competitive nature it is important to model how other players actually play rather than simply assuming the other players will play an arbitrary equilibrium. Using piKL-Hedge, we develop an agent piKL-HedgeBot and show that it improves upon prior approaches. In Appendix B, we also illustrate the key features of piKL-Hedge in Blotto, a famous 2-player simultaneous action game.

4.3.1. BRIEF DESCRIPTION OF DIPLOMACY

In this section, we briefly summarize the rules of Diplomacy. See Paquette et al. (2019) for a more detailed description.

The board is a map of Europe partitioned into 75 regions, 34 of which are *supply centers* (SCs) that players compete for control of. Players command multiple units and each turn privately issues orders for each unit they own (to hold, move, support another unit, convoy, etc) and these orders are revealed at the same time, thereby making Diplomacy a simultaneous-action game. A player wins the game by controlling a majority (18) of the SCs. Diplomacy is specifically designed so that a player is unlikely to achieve victory without help from other players, even though only one player can ultimately win. A game may end in a draw on any turn if all remaining players agree. In this case, we use the **Sum-of-Squares (SoS)** scoring system as used in prior works (Gray et al., 2020; Paquette et al., 2019; Bakhtin et al., 2021). If no player wins, SoS defines the score of player i as $C_i^2 / \sum_i C_i^2$, where C_i is the SC count for player i .

Whereas the full game allows unrestricted private natural-language communication between players to negotiate treaties, share private plans, coordinate actions, etc., we focus on the simpler *no-press* variant, in which no such communication is allowed, but accurately modeling how opponents will behave and choosing actions to coordinate with those of other players continues to be important. Additionally, it still remains possible to signal to other players through actions taken in the game.

4.3.2. DATA AND MODEL ARCHITECTURE

In Diplomacy, we compare the different equilibrium search algorithms (Regret matching, Hedge and piKL-Hedge) using the procedure introduced by Gray et al. (2020). We perform 1-ply lookahead where on each turn, we sample up to 30 of the most likely actions for each player from a policy network trained from on human data. We then consider the 1-ply subgame consisting of those possible actions where the rewards for a given joint action are given by querying a value network trained on human game data as in Gray et al. (2020). We play according to the approximate equilibrium computed for that subgame. For piKL-Hedge, the anchor policy is simply the same human-trained policy network.

Our supervised learning policy model (SL policy) uses the same transformer-encoder architecture as Bakhtin et al. (2021) for reinforcement learning in Diplomacy, but applied to imitation learning instead of RL. We also augment the training data via equivariant permutations of the labels of the players, and further improve the value model by training it to approximate short rollouts of the SL policy. See Appendix E and F for details. We use this SL policy model and improved value model to build an improved SearchBot (Gray et al., 2020), which we call RMBot (Regret-matching bot). We also compare to vanilla unregularized Hedge (Littlestone & Warmuth, 1994; Freund & Schapire, 1997), which we call HedgeBot. piKL-HedgeBot, RMBot and HedgeBot all use

the same SL policy model and improved value model. See Appendix D, for more details about the hyperparameters used in this work.

In Diplomacy, we evaluate piKL-HedgeBot and show that with a particular choice of λ , it predicts human moves as accurately as the underlying SL policy while achieving a much higher head-to-head score. Additionally, a different choice of λ allows for a stronger and more human-like policy than both unregularized search methods.

4.3.3. STRONG, HUMAN-LIKE PLAY WITH PIKL-HEDGE

Similar to Chess and Go, we compare the human prediction accuracy of RMBot, HedgeBot, piKL-HedgeBot (with different λ s) to the SL anchor policy, as well as testing their head-to-head strength. In particular, we test their ability to predict human moves in 226 no-press Diplomacy games from a validation set, and measure their SoS score against the SL policy across 700 games each.

In Figure 4, we present the average top-1 accuracy of unit orders in each action predicted by these methods as well as their average SoS scores against 6 SL anchor policies.

The raw SL model predicts human moves with high accuracy but is weak and achieves low average SoS score. Unregularized search (Hedge and Regret Matching) achieve high average score but low human prediction accuracy.

By contrast, piKL-HedgeBot with different λ achieves a variety of highly favorable combinations of the two. $\lambda = 10^{-1}$ gives about the same top-1 accuracy as the SL policy but with an improvement in score of about 1.4x over the SL anchor policy. $\lambda = 10^{-3}$ outperforms unregularized search methods in both score (by ~5%) and human prediction accuracy (by ~6%). We see mild regularization improves average SoS score, rather than harming it.

As in Chess and Go, we also tested pure RL agents and found they perform poorly in predicting human moves. In particular, the recently proposed DORA and HumanDNVI-NPU algorithms (Bakhtin et al., 2021) achieve top-1 accuracy of only 29.1% and 37.8% respectively.

Next, we compare the top-1 accuracy of these methods across players of different pseudo-Elo ratings. The pseudo-Elos (e_i) for player i is constructed based on the logit rating s_i introduced in Gray et al. (2020), where, $e_i = \frac{s_i \cdot 400}{\log(10)} + 1000$. Figure 5 shows the top-1 accuracy of the different methods for players of different ratings. The top-1 accuracy for all the search based policies increases with pseudo-Elo indicating that they are better at modeling stronger players than weaker players. piKL-Hedge ($\lambda = 10^{-1}$) performs just as well as the anchor policy across pseudo-Elos while being significantly stronger than the anchor, while $\lambda = 10^{-3}$ is as strong or stronger than Hedge and Regret Matching but

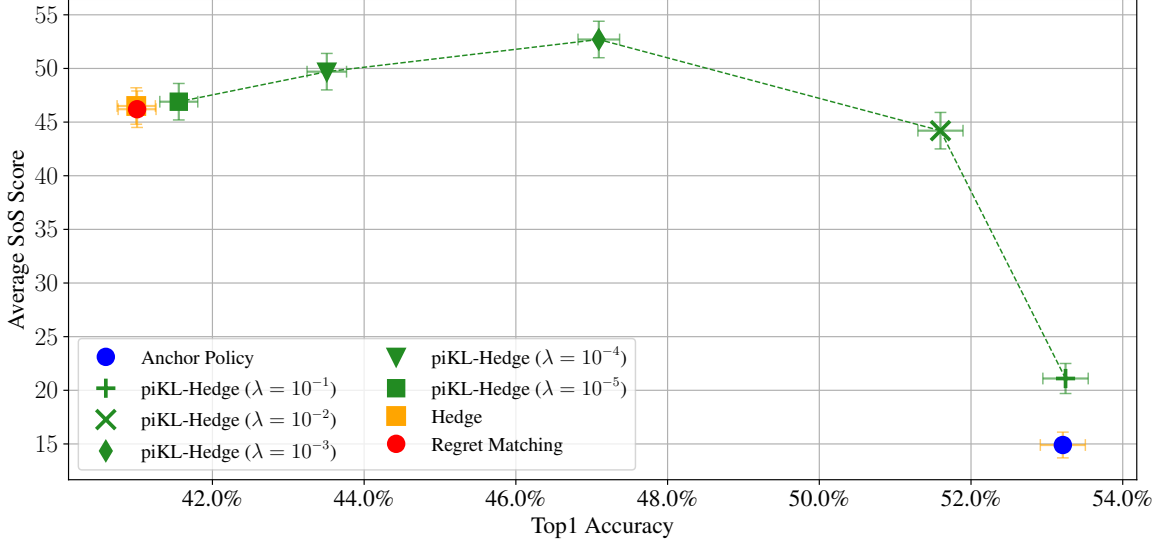


Figure 4. Average top-1 accuracy of unit orders in each action predicted by the human SL anchor policy, regret matching, Hedge and piKL-Hedge and their head to head performance against 6 SL anchor policies. piKL-HedgeBot ($\lambda = 10^{-1}$) predicts human moves as accurately as the anchor policy while achieving a much higher head-to-head performance. At the same time, piKL-HedgeBot ($\lambda = 10^{-3}$) allows for a stronger and more human-like policy than unregularized search methods (hedge, regret matching). Note that equal performance would imply an average SoS score of $1/7 \approx 14.3\%$. Error bars indicate 1 standard error.

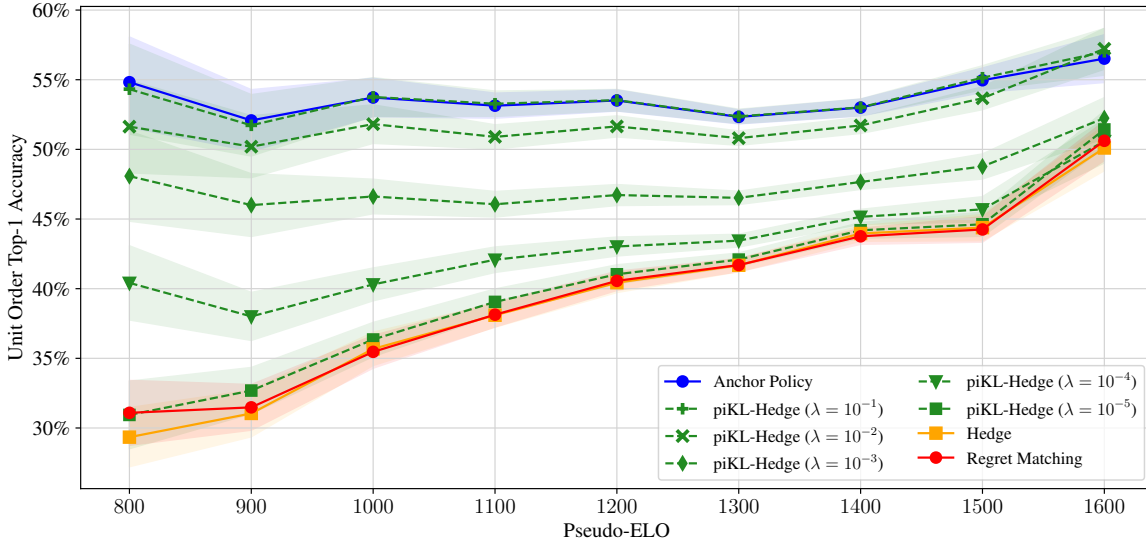


Figure 5. Average top-1 accuracy of unit orders in each action predicted by the human policy, regret matching, and piKL, as a function of pseudo-Elo player rating.

matches human play far better.

In Appendix C, we also show that piKL-Hedge outperforms the unregularized search-based methods by achieving lower average cross-entropy of unit orders. As in chess and Go, KL-regularized search also models the human order distribution well, rather than just the top-1 order.

4.3.4. piKL-HEDGEBOT PERFORMS WELL AGAINST A VARIED POOL OF AGENTS

We also develop a new head-to-head evaluation setting, where rather than testing one agent vs 6x of another agent, all 7 agents per game are sampled uniformly from a pool. The 1v6 head-to-head scores used in prior work (Gray et al., 2020; Bakhtin et al., 2021; Anthony et al., 2020; Paquette

| Agent | Average SoS Score |
|-----------------------------------|-------------------|
| DipNet (Paquette et al., 2019) | 3.7% \pm 0.3% |
| DipNet RL (Paquette et al., 2019) | 4.7% \pm 0.3% |
| Blueprint (Gray et al., 2020) | 4.9% \pm 0.3% |
| BRBot (Gray et al., 2020) | 16.1% \pm 0.6% |
| SearchBot (Gray et al., 2020) | 13.4% \pm 0.5% |
| SL Policy | 7.9% \pm 0.4% |
| RMBot | 31.3% \pm 0.7% |
| piKL-HedgeBot($\lambda = 1e-3$) | 32.9% \pm 0.7% |

Table 4. Average SoS score achieved by agents in a uniformly sampled pool of other agents. piKL-HedgeBot ($\lambda=1e-3$) outperforms all other agents in this setting. DipNet agents from (Paquette et al., 2019) use a temperature of 0.1, while SL Policy and blueprint (Gray et al., 2020) use a temperature of 0.5. The \pm shows one standard error.

et al., 2019) indicate whether a population of 6x agents can be invaded by a 1x agent, and hence whether the 6 agents constitute an Evolutionarily Stable Strategy (ESS) (Taylor & Jonker, 1978; Smith, 1982). By contrast, assigning the 7 agents per game randomly from a pool studies the robustness of an agent to a variety of other agents.

We experiment with a pool of 8 agents. Five are previously published agents: DipNet, DipNet RL (Paquette et al., 2019), Blueprint, BRBot, SearchBot (Gray et al., 2020) and three are our agents: SL policy, RMBot and piKL-HedgeBot. Doing well in this population requires playing well with both human-like policies (DipNet, Blueprint) and equilibrium policies (SearchBot, RMBot). Each experiment only compares one lambda value of piKL-HedgeBot for fairness.

The results of these experiment with piKL-HedgeBot ($\lambda = 10^{-3}$) is presented in Table 4. piKL-HedgeBot ($\lambda = 10^{-3}$) outperforms all other agents. Regularizing towards a human policy allows for stronger play in a population containing human-like agents, while still doing well against equilibrium-searchers in general-sum games like Diplomacy. See Appendix G for results for other λ .

5. Related Work

5.1. Regularized Learning and Planning

Several prior works have explored augmenting reinforcement learning with supervised data from expert demonstrations (Hester et al., 2018; Vecerik et al., 2017; Nair et al., 2018). For example, Hester et al. (2018) augment Deep Q Learning with a margin loss on demonstration data that aims to make $Q(a)$ for the demonstration action higher than that of other actions for each demonstration datapoint. KL-regularized RL has been used as a successful approach

for efficiently incorporating expert demonstrations into the RL training process (Rudner et al., 2021; Ng et al., 2000; Boularias et al., 2011; Wu et al., 2019; Peng et al., 2019; Siegel et al., 2019). In these settings, the standard reinforcement learning objective is augmented by a KL divergence penalty that expresses the dissimilarity between the online policy and a behavioural reference policy derived from demonstrations. This helps guide exploration in RL or ameliorate inaccurate modeling of the environment in domains such as robotics. These works focus on the single agent-environment setting, while we use it as a regularization during inference-time regret minimization search in a multi-agent setting.

AlphaStar (Vinyals et al., 2019), which achieved expert human performance in StarCraft 2, uses self-play reinforcement learning initialized from supervised policies trained to imitate a corpus of human play data. In addition, during the reinforcement learning phase, AlphaStar augments the actor-critic objective with a term that penalizes the KL divergence to the supervised policy at each state encountered during training. However, AlphaStar uses this regularization for RL training while we use it for inference-time search, and AlphaStar uses the regularization to "aid in exploration and to preserve strategic diversity throughout [RL] training", while we use it explicitly to better approximate human play.

The use of entropy-regularized utilities in games is not entirely new. Ling et al. (2018) show that a particular type of entropic regularization in extensive-form games leads to quantal response equilibria. Farina et al. (2019) regularize utilities with a KL divergence term from a pre-computed Nash equilibrium strategy to design agents that trade off game-theoretic safety and exploitation. Cen et al. (2021) give fast online optimization algorithms for entropy-regularized utilities in the context of QRE.

5.2. Human-Compatible Policies

A great deal of prior work in multi-agent reinforcement learning has emphasized the importance of human-compatible policies in cooperative multi-agent environments. Lerer & Peysakhovich (2019) demonstrate that self-play policies may perform poorly with other agents if they do not conform to the population equilibrium (social conventions), and propose a combination of policy gradient and imitation loss directly on samples of population data.

Human-compatible policies have also been studied on the benchmark game of Hanabi, where ad hoc play with humans is regarded as an open challenge problem (Bard et al., 2020). Most work on this challenge has focused on *zero-shot* coordination with humans, in which an agent must adapt to human play with no prior experience with human partners (Hu et al., 2020; 2021; Cui et al., 2021). Learning human-compatible policies from a combination of human data and

planning are less well-studied in this setting.

Prior work on optimizing natural-language communication for a task reward have demonstrated the importance of keeping the policy close to the human data distribution in order to be compatible with human partners. Previous studies (e.g. Lewis et al., 2017; Yarats & Lewis, 2018) have shown that deep network policies for language generation, when directly optimized for a task reward, learn to deploy messages in ways that are inconsistent with their original (natural language) meanings. Several language-specific strategies have been proposed for addressing this problem, including grounding communication in an external modality (Lee et al., 2019), reranking strings according to their probability of correct interpretation (Andreas & Klein, 2016; Vedantam et al., 2017), and population-based training of agents subject to different communicative pressures (Jacob et al., 2021). Lazaridou et al. (2020) introduces a regularization term that encourages generated language to match human corpus data in distribution. Similar to our approach, Jaques et al. (2020) use a KL term to penalize divergence from a prior pre-trained language model during offline RL updates.

5.2.1. IN CHESS AND GO

Chess has been proposed as a setting to study modeling human behavior in the presence of complex multi-step planning and decision making.

MCTS has been a highly studied search method for building strong agents, but both it and other classical search algorithms (e.g. alpha-beta search) have been researched much less in the context of building strong human-like agents. Various authors have had some success in biasing search methods like MCTS to better match human play in minor other domains and applications (Cowling et al., 2015; Khalifa et al., 2016; Baier et al., 2018; Roohi et al., 2021), but prior to our work there appear to be few studies exploring the wider applicability of such methods.

Additionally, notable recent work in chess by McIlroy-Young et al. (2020b) found that MCTS on top of a human imitation-learned model using the default parameters of a standard engine also significantly harmed that model’s human prediction accuracy in chess, but in our work, using a better range of parameters, we show clear results to the contrary. To our knowledge, our work is the first to demonstrate a significant gain in human prediction accuracy over deep learning models via explicit tree search in the highly-studied domains of chess and Go.

5.2.2. IN DIPLOMACY

Diplomacy is a 7-player game that has also been proposed as a major AI challenge (Paquette et al., 2019; Anthony et al., 2020), with a goal of learning how to develop agents capable

of communicating, negotiating, cooperating, and competing in a strategic multi-agent setting. While chess and Go are two-player zero-sum games for which optimal play is well-defined and can be computed through self-play (Nash, 1951), Diplomacy has no such guarantees and strong play requires modeling other agents, even in the no-press variant where natural-language communication is not allowed (Bakhtin et al., 2021; Lerer & Peysakhovich, 2019).

Paquette et al. (2019) showed that with a well-designed neural architecture, imitation learning on human data in no-press Diplomacy can reasonably approximate human play, but that bootstrapping RL from this agent leads to a breakdown in cooperation. Anthony et al. (2020) developed new RL methods based on fictitious play that can improve the performance of supervised agents in no-press Diplomacy, and Gray et al. (2020) showed that an equilibrium-finding regret minimization search procedure on top of human-data-supervised models achieves human-level performance in no-press Diplomacy. However, although both methods rely on the human-supervised model to generate a restricted action set for RL or search, neither contains any explicit regularization to choose among those actions in a way likely to resemble a human player, and we show that the equilibrium search in Gray et al. (2020) greatly decreases the accuracy of modeling human players. Similarly, Bakhtin et al. (2021) achieved strong results in no-press Diplomacy via self-play reinforcement learning both from scratch and initialized with a human-learned policy, but we show also that the resulting final agents do not ultimately predict humans well.

In our work, we show that introducing a KL-regularization term toward the human-learned model to the hedge regret minimization algorithm achieves much higher human prediction accuracy and also improves performance over prior search methods.

6. Conclusion

In this paper, we showed across several domains that regularizing search policies according to a KL-divergence loss with an imitation-learned policy produces policies that maintain high human prediction accuracy while being far stronger than the original learned policy. In chess and Go, applying standard MCTS algorithms regularized towards a human-learned policy predicts human play even better than imitation learning alone, outperforming the prior state-of-the-art prediction accuracy, while also winning more than 85% of games against an agent trained via imitation learning. We then introduced a novel regret minimization algorithm that is regularized based on the KL divergence from an imitation-learned policy. In no-press Diplomacy, this algorithm yields both a policy that predicts human play with the same accuracy as imitation learning alone while increasing win rate against state-of-the-art baselines by a factor of 1.4, or alter-

nately a policy that outperforms unregularized search while achieving much higher human prediction accuracy.

There are several directions for future work. While we extend KL-regularization search to regret minimization in imperfect-information games, it remains to be seen how it would perform when searching beyond just a single move. It is also an open question how this technique could be efficiently extended to belief distributions. Finally, it remains to be seen how KL-regularization search would perform when combined with self-play reinforcement learning.

Author Contributions

A. P. Jacob was the primary researcher for piKL-hedge and contributed to the direction, experiments, and writing of the entire paper. D. J. Wu was the primary researcher for MCTS in chess and Go, and contributed to the direction, experiments, and writing of the entire paper. G. Farina was the primary formulator of the piKL-hedge algorithm and handled all the theory in the paper. A. Lerer contributed to the direction of the project, the formulation of piKL-hedge, its experimental evaluation, and paper writing. A. Bakhtin contributed to the experimental evaluation of piKL-hedge. J. Andreas contributed to the direction of the project and to paper writing. N. Brown initiated the project and contributed to the direction of the project, the formulation of piKL-hedge, its experimental evaluation, and paper writing.

References

- Abernethy, J. and Rakhlin, A. Beating the adaptive bandit with high probability. Technical Report UCB/EECS-2009-10, EECS Department, University of California, Berkeley, Jan 2009. URL <http://www2.eecs.berkeley.edu/Pubs/TechRpts/2009/EECS-2009-10.html>.
- Anderson, A., McIlroy-Young, R., Sen, S., and Kleinberg, J. Introducing maia, a human-like neural network chess engine, 2021. URL <https://lichess.org/blog/X9PUixUAANCqFRSh/introducing-maia-a-human-like-neural-network-chess-engine>.
- Andreas, J. and Klein, D. Reasoning about pragmatics with neural listeners and speakers. In *Proceedings of the 2016 Conference on Empirical Methods in Natural Language Processing*, pp. 1173–1182, 2016.
- Anthony, T., Eccles, T., Tacchetti, A., Kramár, J., Gemp, I., Hudson, T., Porcel, N., Lanctot, M., Perolat, J., Everett, R., Singh, S., Graepel, T., and Bachrach, Y. Learning to play no-press diplomacy with best response policy iteration. In Larochelle, H., Ranzato, M., Hadsell, R., Balcan, M. F., and Lin, H. (eds.), *Advances in Neural Information Processing Systems*, volume 33, pp. 17987–18003. Curran Associates, Inc., 2020. URL <https://proceedings.neurips.cc/paper/2020/file/d1419302db9c022ab1d48681b13d5f8b-Paper.pdf>.
- Baier, H., Sattaur, A., Powley, E., Devlin, S., Rollason, J., and Cowling, P. Emulating human play in a leading mobile card game. *IEEE Transactions on Games*, PP:1–1, 05 2018. doi: 10.1109/TG.2018.2835764.
- Bakhtin, A., Wu, D., Lerer, A., and Brown, N. No-press diplomacy from scratch. In *Thirty-Fifth Conference on Neural Information Processing Systems*, 2021.
- Bard, N., Foerster, J. N., Chandar, S., Burch, N., Lanctot, M., Song, H. F., Parisotto, E., Dumoulin, V., Moitra, S., Hughes, E., et al. The hanabi challenge: A new frontier for ai research. *Artificial Intelligence*, 280:103216, 2020.
- Blackwell, D. et al. An analog of the minimax theorem for vector payoffs. *Pacific Journal of Mathematics*, 6(1):1–8, 1956.
- Boularias, A., Kober, J., and Peters, J. Relative entropy inverse reinforcement learning. In *Proceedings of the Fourteenth International Conference on Artificial Intelligence and Statistics*, pp. 182–189. JMLR Workshop and Conference Proceedings, 2011.
- Brown, N. and Sandholm, T. Superhuman AI for heads-up no-limit poker: Libratus beats top professionals. *Science*, pp. eaao1733, 2017.
- Brown, N. and Sandholm, T. Superhuman AI for multiplayer poker. *Science*, 365(6456):885–890, 2019.
- Campbell, M., Hoane Jr, A. J., and Hsu, F.-h. Deep Blue. *Artificial intelligence*, 134(1-2):57–83, 2002.
- Cazenave, T. Residual networks for computer go. *IEEE Transactions on Computational Intelligence and AI in Games*, PP:1–1, 03 2017. doi: 10.1109/TCIAIG.2017.2681042.
- Cen, S., Wei, Y., and Chi, Y. Fast policy extragradient methods for competitive games with entropy regularization. In *Neural Information Processing Systems (NeurIPS)*, 2021.
- Cowling, P., Devlin, S., Powley, E., Whitehouse, D., and Rollason, J. Player preference and style in a leading mobile card game. *IEEE Transactions on Computational Intelligence and AI in Games*, 7:233–242, 2015.
- Cui, B., Hu, H., Pineda, L., and Foerster, J. K-level reasoning for zero-shot coordination in hanabi. In *Thirty-Fifth Conference on Neural Information Processing Systems*, 2021.

- Egri-Nagy, A. and Törmänen, A. The game is not over yet—go in the post-alphago era. *Philosophies*, 5(4):37–0, 2020. ISSN 2409-9287. doi: 10.3390/philosophies5040037. URL <https://www.mdpi.com/2409-9287/5/4/37>.
- Farina, G., Kroer, C., and Sandholm, T. Online convex optimization for sequential decision processes and extensive-form games. In *AAAI Conference on Artificial Intelligence*, 2019.
- Freund, Y. and Schapire, R. E. A decision-theoretic generalization of on-line learning and an application to boosting. *Journal of computer and system sciences*, 55(1):119–139, 1997.
- Gray, J., Lerer, A., Bakhtin, A., and Brown, N. Human-level performance in no-press diplomacy via equilibrium search. In *International Conference on Learning Representations*, 2020.
- Grill, J.-B., Altché, F., Tang, Y., Hubert, T., Valko, M., Antonoglou, I., and Munos, R. Monte-carlo tree search as regularized policy optimization. In *International Conference on Machine Learning*, pp. 3769–3778. PMLR, 2020.
- Hannan, J. Approximation to bayes risk in repeated play. *Contributions to the Theory of Games*, 3:97–139, 1957.
- Hart, S. and Mas-Colell, A. A simple adaptive procedure leading to correlated equilibrium. *Econometrica*, 68(5): 1127–1150, 2000.
- Hester, T., Vecerik, M., Pietquin, O., Lanctot, M., Schaul, T., Piot, B., Horgan, D., Quan, J., Sendonaris, A., Osband, I., et al. Deep q-learning from demonstrations. In *Thirty-second AAAI conference on artificial intelligence*, 2018.
- Hu, H., Lerer, A., Peysakhovich, A., and Foerster, J. “other-play” for zero-shot coordination. In *International Conference on Machine Learning*, pp. 4399–4410. PMLR, 2020.
- Hu, H., Lerer, A., Cui, B., Pineda, L., Wu, D., Brown, N., and Foerster, J. Off-belief learning. In *International Conference on Machine Learning*. PMLR, 2021.
- Hu, J., Shen, L., and Sun, G. Squeeze-and-excitation networks. In *2018 IEEE/CVF Conference on Computer Vision and Pattern Recognition*, pp. 7132–7141, 2018. doi: 10.1109/CVPR.2018.00745.
- Jacob, A. P., Lewis, M., and Andreas, J. Multitasking inhibits semantic drift. In *Proceedings of the 2021 Conference of the North American Chapter of the Association for Computational Linguistics: Human Language Technologies*, pp. 5351–5366, 2021.
- Jaques, N., Shen, J. H., Ghandeharioun, A., Ferguson, C., Lapedriza, A., Jones, N., Gu, S., and Picard, R. Human-centric dialog training via offline reinforcement learning. In *Proceedings of the 2020 Conference on Empirical Methods in Natural Language Processing (EMNLP)*, pp. 3985–4003, 2020.
- Khalifa, A., Isaksen, A., Togelius, J., and Nealen, A. Modifying mcts for human-like general video game playing. In *IJCAI*, 2016.
- Lai, M. Forum post on alphazero news (post by user matthewlai). <http://talkchess.com/forum3/viewtopic.php?f=2&t=69175&sid=06ca6a966c29743d765c11b13402be8d&start=70#p781765>, 2018.
- Lazaridou, A., Potapenko, A., and Tieleman, O. Multi-agent communication meets natural language: Synergies between functional and structural language learning. In *Proceedings of the 58th Annual Meeting of the Association for Computational Linguistics*, pp. 7663–7674, 2020.
- LC0. Leela chess zero information page on "neural network topology". <https://lczero.org/dev/backend/nn/>, 2020.
- Lee, J., Cho, K., and Kiela, D. Countering language drift via visual grounding. In *Proceedings of the 2019 Conference on Empirical Methods in Natural Language Processing and the 9th International Joint Conference on Natural Language Processing (EMNLP-IJCNLP)*, pp. 4376–4386, 2019.
- Lerer, A. and Peysakhovich, A. Learning existing social conventions via observationally augmented self-play. In *Proceedings of the 2019 AAAI/ACM Conference on AI, Ethics, and Society*, pp. 107–114. ACM, 2019.
- Lewis, M., Yarats, D., Dauphin, Y., Parikh, D., and Batra, D. Deal or no deal? end-to-end learning of negotiation dialogues. In *Proceedings of the 2017 Conference on Empirical Methods in Natural Language Processing*, pp. 2443–2453, 2017.
- Ling, C. K., Fang, F., and Kolter, J. Z. What game are we playing? end-to-end learning in normal and extensive form games. *International Joint Conferences on Artificial Intelligence Organization*, 2018.
- Littlestone, N. and Warmuth, M. K. The weighted majority algorithm. *Information and computation*, 108(2):212–261, 1994.
- McIlroy-Young, R., Sen, S., Kleinberg, J., and Anderson, A. Aligning superhuman ai with human behavior: Chess as a model system. In *Proceedings of the 26th ACM SIGKDD International Conference on Knowledge Discovery & Data Mining*, pp. 1677–1687, 2020a.

- McIlroy-Young, R., Wang, R., Sen, S., Kleinberg, J., and Anderson, A. Learning personalized models of human behavior in chess. Technical report, Microsoft, Inc., August 2020b. URL <https://www.microsoft.com/en-us/research/publication/learning-personalized-models-of-human-behavior-in-chess/>.
- McKelvey, R. D. and Palfrey, T. R. Quantal response equilibria for normal form games. *Games and Economic Behavior*, 10(1):6–38, 1995a. ISSN 0899-8256. doi: <https://doi.org/10.1006/game.1995.1023>. URL <https://www.sciencedirect.com/science/article/pii/S0899825685710238>.
- McKelvey, R. D. and Palfrey, T. R. Quantal response equilibria for normal form games. *Games and economic behavior*, 10(1):6–38, 1995b.
- Moravčík, M., Schmid, M., Burch, N., Lisý, V., Morrill, D., Bard, N., Davis, T., Waugh, K., Johanson, M., and Bowling, M. Deepstack: Expert-level artificial intelligence in heads-up no-limit poker. *Science*, 356(6337):508–513, 2017.
- Nair, A., McGrew, B., Andrychowicz, M., Zaremba, W., and Abbeel, P. Overcoming exploration in reinforcement learning with demonstrations. In *2018 IEEE International Conference on Robotics and Automation (ICRA)*, pp. 6292–6299. IEEE, 2018.
- Nash, J. Non-cooperative games. *Annals of mathematics*, pp. 286–295, 1951.
- Ng, A. Y., Russell, S. J., et al. Algorithms for inverse reinforcement learning. In *Icml*, volume 1, pp. 2, 2000.
- Paquette, P., Lu, Y., Bocco, S. S., Smith, M., Satya, O.-G., Kummerfeld, J. K., Pineau, J., Singh, S., and Courville, A. C. No-press diplomacy: Modeling multi-agent gameplay. In *Advances in Neural Information Processing Systems*, pp. 4474–4485, 2019.
- Peng, X. B., Kumar, A., Zhang, G., and Levine, S. Advantage-weighted regression: Simple and scalable off-policy reinforcement learning. *arXiv preprint arXiv:1910.00177*, 2019.
- Rakhlin, A. Lecture notes on online learning, 2009.
- Roohi, S., Guckelsberger, C., Relas, A., Heiskanen, H., Takatalo, J., and Hämmäläinen, P. Predicting game engagement and difficulty using AI players. *CoRR*, abs/2107.12061, 2021. URL <https://arxiv.org/abs/2107.12061>.
- Rudner, T. G., Lu, C., Osborne, M., Gal, Y., and Teh, Y. W. On pathologies in kl-regularized reinforcement learning from expert demonstrations. In *Thirty-Fifth Conference on Neural Information Processing Systems*, 2021.
- Schrittwieser, J., Antonoglou, I., Hubert, T., Simonyan, K., Sifre, L., Schmitt, S., Guez, A., Lockhart, E., Hassabis, D., Graepel, T., et al. Mastering atari, go, chess and shogi by planning with a learned model. *Nature*, 588(7839): 604–609, 2020.
- Siegel, N., Springenberg, J. T., Berkenkamp, F., Abdolmaleki, A., Neunert, M., Lampe, T., Hafner, R., Heess, N., and Riedmiller, M. Keep doing what worked: Behavior modelling priors for offline reinforcement learning. In *International Conference on Learning Representations*, 2019.
- Silver, D., Huang, A., Maddison, C. J., Guez, A., Sifre, L., Van Den Driessche, G., Schrittwieser, J., Antonoglou, I., Panneershelvam, V., Lanctot, M., et al. Mastering the game of go with deep neural networks and tree search. *Nature*, 529(7587):484, 2016.
- Silver, D., Schrittwieser, J., Simonyan, K., Antonoglou, I., Huang, A., Guez, A., Hubert, T., Baker, L., Lai, M., Bolton, A., et al. Mastering the game of go without human knowledge. *Nature*, 550(7676):354, 2017.
- Silver, D., Hubert, T., Schrittwieser, J., Antonoglou, I., Lai, M., Guez, A., Lanctot, M., Sifre, L., Kumaran, D., Graepel, T., et al. A general reinforcement learning algorithm that masters chess, shogi, and go through self-play. *Science*, 362(6419):1140–1144, 2018.
- Smith, J. M. *Evolution and the Theory of Games*. Cambridge university press, 1982.
- Taylor, P. D. and Jonker, L. B. Evolutionary stable strategies and game dynamics. *Mathematical biosciences*, 40(1-2): 145–156, 1978.
- Tian, Y. Github thread for elf opengo, "[suggestion] clarify fpu in paper". <https://github.com/pytorch/ELF/issues/140>, 2019.
- Troisi, S. Github thread for minigo "[experiment] squeeze and excitation". <https://github.com/tensorflow/minigo/issues/683>, 2019.
- Vecerik, M., Hester, T., Scholz, J., Wang, F., Pietquin, O., Piot, B., Heess, N., Rothörl, T., Lampe, T., and Riedmiller, M. Leveraging demonstrations for deep reinforcement learning on robotics problems with sparse rewards. *arXiv preprint arXiv:1707.08817*, 2017.
- Vedantam, R., Bengio, S., Murphy, K., Parikh, D., and Chechik, G. Context-aware captions from context-agnostic supervision. In *Proceedings of the IEEE Conference on Computer Vision and Pattern Recognition*, pp. 251–260, 2017.

Vinyals, O., Babuschkin, I., Czarnecki, W. M., Mathieu, M., Dudzik, A., Chung, J., Choi, D. H., Powell, R., Ewalds, T., Georgiev, P., et al. Grandmaster level in starcraft ii using multi-agent reinforcement learning. *Nature*, 575 (7782):350–354, 2019.

Wu, D. Go neural net sandbox. <https://github.com/lightvector/GoNN#raw-neural-net-results>, 2018.

Wu, D. Accelerating self-play learning in go. In *AAAI-20 Workshop on Reinforcement Learning in Games*, 2020.

Wu, Y., Tucker, G., and Nachum, O. Behavior regularized offline reinforcement learning. 2019.

Yarats, D. and Lewis, M. Hierarchical text generation and planning for strategic dialogue. In *Proceedings of the 35th International Conference on Machine Learning, ICML 2018, Stockholmsmässan, Stockholm, Sweden, July 10-15, 2018*, pp. 5587–5595, 2018.

A. Proofs

In this Appendix, we present detailed proofs of Proposition 1 and Theorem 2.

A.1. Known results

We start by recalling a few standard results. First, we recall the follow-the-regularized-leader (FTRL) algorithm, one of the most well-studied algorithms in online optimization. At every time t , the FTRL algorithm instantiated with domain \mathcal{X} , 1-strongly-convex regularizer $\phi : \mathcal{X} \rightarrow \mathbb{R}$, and learning rate $\eta > 0$, produces iterates according to

$$\mathbf{x}^{t+1} = \arg \max_{\mathbf{x} \in \mathcal{X}} \left\{ -\frac{\phi(\mathbf{x})}{\eta} + \sum_{\tau=1}^t \ell^\tau(\mathbf{x}) \right\}, \quad (\text{FTRL})$$

where ℓ^1, \dots, ℓ^t are the convex utility functions gave as feedback by the environment. The FTRL algorithm guarantees the following regret bound.

Lemma 1 (Rakhlin (2009), Corollary 7). *The iterates $\mathbf{x}^t \in \mathcal{X}$ produced by the FTRL algorithm set up with constant step size $\eta > 0$ and 1-strongly convex regularizer ϕ satisfy the regret bound*

$$\sum_{t=1}^T \ell^t(\mathbf{u}) - \ell^t(\mathbf{x}^t) \leq \frac{\phi(\mathbf{u})}{\eta} + \sum_{t=1}^T \ell^t(\mathbf{x}^{t+1}) - \ell^t(\mathbf{x}^t) \quad \forall \mathbf{u} \in \mathcal{X}. \quad (9)$$

In the analysis of Algorithm 1 we will also make use of the following technical lemma, a proof of which can be obtained starting using the same techniques as Abernethy & Rakhlin (2009, Lemma A.4)

Lemma 2. *Let $\mathbf{p} \in \Delta(A)$ be a distribution over a discrete set A , $\mathbf{q} \in \mathbb{R}^{|A|}$ be a vector, and $D > 0$ be any constant such that $\max_{a, a' \in A} \{\mathbf{q}(a) - \mathbf{q}(a')\} \leq D$. Then,*

$$\frac{\sum_{a \in A} \mathbf{p}(a) \cdot \exp\{-\mathbf{q}(a)\}^2}{\left(\sum_{a \in A} \mathbf{p}(a) \cdot \exp\{-\mathbf{q}(a)\}\right)^2} - 1 \leq \frac{\exp\{2D\}}{D^2} \sum_{a \in A} \mathbf{p}(a) \mathbf{q}(a)^2.$$

Proof. Let $q_{\min} := \min_{a \in A} \mathbf{q}(a)$ and $\tilde{\mathbf{q}}(a) := \mathbf{q}(a) - q_{\min}$ be a shifted version of $\mathbf{q}(a)$ so that $0 \leq \tilde{\mathbf{q}}(a) \leq D$ for all $a \in A$. Let now X denote a random variable with value $\tilde{\mathbf{q}}(a)$ with probability $\mathbf{p}(a)$ for all $a \in A$. Then,

$$\begin{aligned} \frac{\sum_{a \in A} \mathbf{p}(a) \cdot \exp\{-\mathbf{q}(a)\}^2}{\left(\sum_{a \in A} \mathbf{p}(a) \cdot \exp\{-\mathbf{q}(a)\}\right)^2} - 1 &= \frac{\exp\{q_{\min}\}^2 \sum_{a \in A} \mathbf{p}(a) \cdot \exp\{\tilde{\mathbf{q}}(a)\}^2}{\exp\{q_{\min}\}^2 \left(\sum_{a \in A} \mathbf{p}(a) \cdot \exp\{-\mathbf{q}(a)\}\right)^2} - 1 \\ &= \frac{\sum_{a \in A} \mathbf{p}(a) \cdot \exp\{-\tilde{\mathbf{q}}(a)\}^2}{\left(\sum_{a \in A} \mathbf{p}(a) \cdot \exp\{-\tilde{\mathbf{q}}(a)\}\right)^2} - 1 \\ &= \frac{\mathbb{E}[\exp(-X)]}{[\mathbb{E} \exp(-X)]^2} - 1. \end{aligned}$$

Applying Lemma A.4 from Abernethy & Rakhlin (2009) we obtain

$$\frac{\sum_{a \in A} \mathbf{p}(a) \cdot \exp\{-\mathbf{q}(a)\}^2}{\left(\sum_{a \in A} \mathbf{p}(a) \cdot \exp\{-\mathbf{q}(a)\}\right)^2} - 1 \leq \frac{\exp\{2D\} - 2D - 1}{D^2} (\mathbb{E}[X^2] - \mathbb{E}[X]^2) \leq \frac{\exp\{2D\}}{D^2} \mathbb{E}[X^2],$$

which is exactly the statement. \square

A.2. Bounding the distance between the iterates of Algorithm 1

Lemma 3. *At all times t and for all players i , the policies π_i^t produced by the FTRL algorithm set up with constant step size η and negative entropy regularizer $\varphi(\mathbf{x}) := \sum_{a \in A_i} \mathbf{x}(a) \log \mathbf{x}(a)$, when observing the utilities \mathcal{U}_i^t , match the policies π_i^t produced by Algorithm 1.*

Proof. Plugging the particular choices of utilities and regularizer into (FTRL), we obtain

$$\begin{aligned}
 \pi_i^{t+1} &= \arg \max_{\pi \in \Delta(A_i)} \left\{ \left(\sum_{t'=1}^t \mathcal{U}_i^{t'}(\pi) \right) - \frac{1}{\eta} \sum_{a \in A_i} \pi(a) \log \pi(a) \right\} \\
 &= \arg \max_{\pi \in \Delta(A_i)} \left\{ \eta \left(\sum_{t'=1}^t \sum_{a \in A_i} \pi(a) u_i(a, \mathbf{a}_{-i}^{t'}) - \lambda_i \pi(a) \log \left(\frac{\pi(a)}{\tau_i(a)} \right) \right) - \sum_{a \in A_i} \pi(a) \log \pi(a) \right\} \\
 &= \arg \max_{\pi \in \Delta(A_i)} \left\{ \eta \sum_{a \in A_i} \left(t \lambda_i \log \tau_i(a) + \sum_{t'=1}^t u_i(a, \mathbf{a}_{-i}^{t'}) \right) \pi(a) - (1 + t \lambda_i \eta) \sum_{a \in A_i} \pi(a) \log \pi(a) \right\} \\
 &= \arg \max_{\pi \in \Delta(A_i)} \left\{ \frac{\eta}{1 + t \lambda_i \eta} \sum_{a \in A_i} \left(t \lambda_i \log \tau_i(a) + \sum_{t'=1}^t u_i(a, \mathbf{a}_{-i}^{t'}) \right) \pi(a) - \sum_{a \in A_i} \pi(a) \log \pi(a) \right\}. \tag{10}
 \end{aligned}$$

A well-known closed form solution to the above entropy-regularized problem is given by the softmax function. In particular, let

$$\mathbf{w}_i^{t+1}(a) := \frac{\eta}{1 + t \lambda_i \eta} \left(t \lambda_i \log \tau_i(a) + \sum_{t'=1}^t \tilde{u}_i(a, \mathbf{a}_{-i}^{t'}) \right) \quad \forall a \in A_i. \tag{11}$$

Then,

$$\pi_i^{t+1}(a) = \frac{\exp\{\mathbf{w}_i^{t+1}(a)\}}{\sum_{a' \in A_i} \exp\{\mathbf{w}_i^{t+1}(a')\}} \quad \forall a \in A_i,$$

which coincides with the iterate produced by Algorithm 1. \square

The next observation shows that the iterates π_i do not change if the utility function u_i is first shifted to be in the range $[0, D_i]$.

Remark 1. Consider the shifted utilities

$$\tilde{u}_i(a, \mathbf{a}_{-i}^t) := u_i(a, \mathbf{a}_{-i}^t) - \min_{\mathbf{a} \in A_1 \times \dots \times A_n} u_i(\mathbf{a}) \in [0, D_i] \tag{12}$$

and let \mathbf{v} be defined as (11) using \tilde{u}_i in place of u_i , that is,

$$\mathbf{v}_i^{t+1}(a) := \frac{\eta}{1 + t \lambda_i \eta} \left(t \lambda_i \log \tau_i(a) + \sum_{t'=1}^t \tilde{u}_i(a, \mathbf{a}_{-i}^{t'}) \right) \quad \forall a \in A_i. \tag{13}$$

Then, the iterates π_i can be equivalently expressed as

$$\pi_i^{t+1}(a) = \frac{\exp\{\mathbf{v}_i^{t+1}(a)\}}{\sum_{a' \in A_i} \exp\{\mathbf{v}_i^{t+1}(a')\}} \quad \forall a \in A_i.$$

Proof. Let $\gamma :=$

$\min_{\mathbf{a} \in A_1 \times \dots \times A_n} u_i(\mathbf{a})$ denote the minimum utility that Player i can get against the actions of the opponents. Since the argmax of a function does not change if a constant is added to the objective, from (10) we can write

$$\begin{aligned}
 \pi_i^{t+1} &= \arg \max_{\pi \in \Delta(A_i)} \left\{ -\frac{\eta}{1 + t \lambda_i \eta} \gamma + \frac{\eta}{1 + t \lambda_i \eta} \sum_{a \in A_i} \left(t \lambda_i \log \tau_i(a) + \sum_{t'=1}^t u_i(a, \mathbf{a}_{-i}^{t'}) \right) \pi(a) - \sum_{a \in A_i} \pi(a) \log \pi(a) \right\} \\
 &= \arg \max_{\pi \in \Delta(A_i)} \left\{ \frac{\eta}{1 + t \lambda_i \eta} \sum_{a \in A_i} \left(t \lambda_i \log \tau_i(a) + \sum_{t'=1}^t (u_i(a, \mathbf{a}_{-i}^{t'}) - \gamma) \right) \pi(a) - \sum_{a \in A_i} \pi(a) \log \pi(a) \right\} \\
 &= \arg \max_{\pi \in \Delta(A_i)} \left\{ \sum_{a \in A_i} \mathbf{v}_i^{t+1}(a) \pi(a) - \sum_{a \in A_i} \pi(a) \log \pi(a) \right\},
 \end{aligned}$$

where the second equality follows from the fact that $\pi \in \Delta(A_i)$.

A solution is again given by softmax function

$$\pi_i^{t+1}(a) = \frac{\exp\{\mathbf{v}_i^{t+1}(a)\}}{\sum_{a' \in A_i} \exp\{\mathbf{v}_i^{t+1}(a')\}} \quad \forall a \in A_i. \quad (14)$$

□

In the rest of the proof we will use (14) to analyze the iterates π_i produced by the algorithm.

Lemma 4. *Let $\eta \leq 1/(\lambda_i \beta_i + 2D_i)$. Then, at all times t ,*

$$\|\pi_i^{t+1} - \pi_i^t\|_{\nabla^2 \varphi(\pi_i^t)} \leq \frac{\sqrt{3}e}{t\lambda_i\eta}.$$

Proof. At all times t , introduce the vector $\xi_i^t \in \mathbb{R}^{|A_i|}$ defined as

$$\xi_i^t(a) := \frac{\eta}{1 + t\lambda_i\eta} (-\lambda_i \mathbf{v}^t(a) + \lambda_i \log \tau_i(a) + \tilde{u}_i(a, \mathbf{a}_{-i}^t)) \quad \forall a \in A_i. \quad (15)$$

At all times t and for all a , it holds that

$$\begin{aligned} \mathbf{v}_i^{t+1}(a) &= \frac{\eta}{1 + t\lambda_i\eta} \left(\frac{1 + (t-1)\lambda_i\eta}{\eta} \mathbf{v}^t(a) + \lambda_i \log \tau_i(a) + \tilde{u}_i(a, \mathbf{a}_{-i}^t) \right) \\ &= \frac{\eta}{1 + t\lambda_i\eta} \left(\frac{1 + t\lambda_i\eta}{\eta} \mathbf{v}^t(a) - \lambda_i \mathbf{v}^t(a) + \lambda_i \log \tau_i(a) + \tilde{u}_i(a, \mathbf{a}_{-i}^t) \right) \\ &= \mathbf{v}^t(a) + \xi_i^t(a). \end{aligned} \quad (16)$$

Substituting (16) we can write

$$\pi_i^{t+1}(a) = \frac{\exp\{\mathbf{v}_i^t(a)\} \cdot \exp\{\xi_i^t(a)\}}{\sum_{a' \in A_i} \exp\{\mathbf{v}_i^t(a')\} \cdot \exp\{\xi_i^t(a')\}} = \frac{\pi_i^t(a) \exp\{\xi_i^t(a)\}}{\sum_{a' \in A_i} \pi_i^t(a') \exp\{\xi_i^t(a')\}}. \quad (17)$$

Expanding the definition of the local norm induced by $\nabla^2 \varphi(\pi_i^t)$ we find

$$\begin{aligned} \|\pi_i^{t+1} - \pi_i^t\|_{\nabla^2 \varphi(\pi_i^t)}^2 &= \sum_{a \in A_i} \frac{1}{\pi_i^t(a)} (\pi_i^{t+1}(a) - \pi_i^t(a))^2 \\ &= \sum_{a \in A_i} \pi_i^t(a) \left(\frac{\exp\{\xi_i^t(a)\}}{\sum_{a' \in A_i} \pi_i^t(a') \exp\{\xi_i^t(a')\}} - 1 \right)^2 \end{aligned} \quad (18)$$

$$\begin{aligned} &= \sum_{a \in A_i} \pi_i^t(a) \left[\left(\frac{\exp\{\xi_i^t(a)\}}{\sum_{a' \in A_i} \pi_i^t(a') \exp\{\xi_i^t(a')\}} \right)^2 - 2 \left(\frac{\exp\{\xi_i^t(a)\}}{\sum_{a' \in A_i} \pi_i^t(a') \exp\{\xi_i^t(a')\}} \right) + 1 \right] \\ &= \frac{\sum_{a \in A_i} \pi_i^t(a) \exp\{\xi_i^t(a)\}^2}{\left(\sum_{a' \in A_i} \pi_i^t(a') \exp\{\xi_i^t(a')\} \right)^2} - 2 \frac{\sum_{a \in A_i} \pi_i^t(a) \exp\{\xi_i^t(a)\}}{\sum_{a' \in A_i} \pi_i^t(a') \exp\{\xi_i^t(a')\}} + \sum_{a \in A_i} \pi_i^t(a) \\ &= \frac{\sum_{a \in A_i} \pi_i^t(a) \exp\{\xi_i^t(a)\}^2}{\left(\sum_{a' \in A_i} \pi_i^t(a') \exp\{\xi_i^t(a')\} \right)^2} - 1, \end{aligned} \quad (19)$$

where (18) follows from substituting (17). We now apply Lemma 2, applied with $\mathbf{q} = \xi_i^t$, $\mathbf{p} = \pi_i^t$, and $A = A_i$. First, we study the range $D_i = \max_{a, a' \in A_i} \{\xi_i^t(a) - \xi_i^t(a')\}$ used in the statement of the Lemma. In particular, using (16) we have

$$\begin{aligned} \max_{a, a' \in A_i} \{\xi_i^t(a) - \xi_i^t(a')\} &= \max_{a, a' \in A_i} \{\mathbf{v}_i^{t+1}(a) - \mathbf{v}_i^t(a) - \mathbf{v}_i^{t+1}(a') + \mathbf{v}_i^t(a')\} \\ &= \max_{a, a' \in A_i} \left\{ (\log \tau_i(a) - \log \tau_i(a')) \cdot \left(\frac{t\lambda_i\eta}{1 + t\lambda_i\eta} - \frac{(t-1)\lambda_i\eta}{1 + (t-1)\lambda_i\eta} \right) \right\} \end{aligned}$$

$$\begin{aligned}
 & + \frac{\eta}{1+t\lambda_i\eta} \left(\sum_{t'=1}^t \tilde{u}_i(a, \mathbf{a}_{-i}^{t'}) - \tilde{u}_i(a', \mathbf{a}_{-i}^{t'}) \right) \\
 & - \frac{\eta}{1+(t-1)\lambda_i\eta} \left(\sum_{t'=1}^{t-1} \tilde{u}_i(a, \mathbf{a}_{-i}^{t'}) - \tilde{u}_i(a', \mathbf{a}_{-i}^{t'}) \right) \Bigg\} \\
 & = \max_{a, a' \in A_i} \left\{ \frac{\lambda_i\eta}{(1+t\lambda_i\eta)(1+(t-1)\lambda_i\eta)} (\log \tau_i(a) - \log \tau_i(a')) \right. \\
 & \quad + \frac{\lambda_i\eta^2}{(1+t\lambda_i\eta)(1+(t-1)\lambda_i\eta)} \left(\sum_{t'=1}^{t-1} \tilde{u}_i(a, \mathbf{a}_{-i}^{t'}) - \tilde{u}_i(a', \mathbf{a}_{-i}^{t'}) \right) \\
 & \quad \left. + \frac{\eta}{1+t\lambda_i\eta} (\tilde{u}_i(a, \mathbf{a}_{-i}^t) - \tilde{u}_i(a', \mathbf{a}_{-i}^t)) \right\} \\
 & \leq \max_{a, a' \in A_i} \left\{ \frac{\lambda_i\eta}{(1+t\lambda_i\eta)(1+(t-1)\lambda_i\eta)} (\log \tau_i(a) - \log \tau_i(a')) \right\} \\
 & \quad + \max_{a, a' \in A_i} \left\{ \frac{\lambda_i\eta^2}{(1+t\lambda_i\eta)(1+(t-1)\lambda_i\eta)} \left(\sum_{t'=1}^{t-1} \tilde{u}_i(a, \mathbf{a}_{-i}^{t'}) - \tilde{u}_i(a', \mathbf{a}_{-i}^{t'}) \right) \right\} \\
 & \quad + \max_{a, a' \in A_i} \left\{ \frac{\eta}{1+t\lambda_i\eta} (\tilde{u}_i(a, \mathbf{a}_{-i}^t) - \tilde{u}_i(a', \mathbf{a}_{-i}^t)) \right\} \\
 & \leq \eta(\lambda_i\beta_i + 2D_i), \tag{20}
 \end{aligned}$$

where the first inequality follows from upper bounding the max of a sum with the sum of max of each term, and the second inequality follows from noting that

$$\frac{\lambda_i\eta}{(1+t\lambda_i\eta)(1+(t-1)\lambda_i\eta)} \leq \frac{\eta}{1+t\lambda_i\eta} \leq \eta,$$

and

$$\frac{\lambda_i\eta^2}{(1+t\lambda_i\eta)(1+(t-1)\lambda_i\eta)} \leq \frac{\eta}{t} \left(\sum_{t'=1}^{t-1} \tilde{u}_i(a, \mathbf{a}_{-i}^{t'}) - \tilde{u}_i(a', \mathbf{a}_{-i}^{t'}) \right) \leq \frac{\lambda_i\eta^2}{t\lambda_i\eta} \cdot tD_i = \eta D_i.$$

Applying Lemma 2 to the right-hand side of (19) using the bound on the range of ξ_i^t shown in (20) yields

$$\|\pi_i^{t+1} - \pi_i^t\|_{\nabla^2 \varphi(\pi_i^t)}^2 \leq \frac{\exp\{2\eta(\lambda_i\beta_i + 2D_i)\}}{\eta^2(\lambda_i\beta_i + 2D_i)^2} \sum_{a \in A_i} \pi_i^t(a) (\xi_i^t(a))^2. \tag{21}$$

Using the fact that any convex combination of values is upper bounded by the maximum value, we can further bound the right-hand side of (21) as

$$\begin{aligned}
 \|\pi_i^{t+1} - \pi_i^t\|_{\nabla^2 \varphi(\pi_i^t)}^2 & \leq \frac{\exp\{2\eta(\lambda_i\beta_i + 2D_i)\}}{\eta^2(\lambda_i\beta_i + 2D_i)^2} \max_{a \in A_i} (\xi_i^t(a))^2 \\
 & = \frac{\exp\{2\eta(\lambda_i\beta_i + 2D_i)\}}{\eta^2(\lambda_i\beta_i + 2D_i)^2} \max_{a \in A_i} (v_i^{t+1}(a) - v_i^t(a))^2,
 \end{aligned}$$

where the equality follows from (16). Hence, expanding the definition of v_i^t and v_i^{t+1} ,

$$\begin{aligned}
 \|\pi_i^{t+1} - \pi_i^t\|_{\nabla^2 \varphi(\pi_i^t)}^2 & \leq \frac{\exp\{2\eta(\lambda_i\beta_i + 2D_i)\}}{\eta^2(\lambda_i\beta_i + 2D_i)^2} \max_{a \in A_i} \left\{ \left(\frac{t\lambda_i\eta}{1+t\lambda_i\eta} - \frac{(t-1)\lambda_i\eta}{1+(t-1)\lambda_i\eta} \right) \log \tau_i(a) \right. \\
 & \quad \left. + \frac{\eta}{1+t\lambda_i\eta} \sum_{t'=1}^t \tilde{u}_i(a, \mathbf{a}_{-i}^{t'}) - \frac{\eta}{1+(t-1)\lambda_i\eta} \sum_{t'=1}^{t-1} \tilde{u}_i(a, \mathbf{a}_{-i}^{t'}) \right\}^2 \\
 & = \frac{\exp\{2\eta(\lambda_i\beta_i + 2D_i)\}}{\eta^2(\lambda_i\beta_i + 2D_i)^2} \max_{a \in A_i} \left\{ \frac{\lambda_i\eta}{(1+t\lambda_i\eta)(1+(t-1)\lambda_i\eta)} \log \tau_i(a) + \frac{\eta}{1+t\lambda_i\eta} \tilde{u}_i(a, \mathbf{a}_{-i}^t) \right. \\
 & \quad \left. - \frac{\eta}{1+(t-1)\lambda_i\eta} \tilde{u}_i(a, \mathbf{a}_{-i}^{t-1}) \right\}^2
 \end{aligned}$$

$$\begin{aligned}
 & - \frac{\lambda_i \eta^2}{(1 + t\lambda_i \eta)(1 + (t-1)\lambda_i \eta)} \sum_{t'=1}^{t-1} \tilde{u}_i(a, \mathbf{a}_{-i}^{t'}) \Big\}^2 \\
 & \leq 3 \frac{\exp\{2\eta(\lambda_i \beta_i + 2D_i)\}}{\eta^2(\lambda_i \beta_i + 2D_i)^2} \max_{a \in A_i} \left\{ \left(\frac{\lambda_i \eta}{(1 + t\lambda_i \eta)(1 + (t-1)\lambda_i \eta)} \log \tau_i(a) \right)^2 + \left(\frac{\eta}{1 + t\lambda_i \eta} \tilde{u}_i(a, \mathbf{a}_{-i}^t) \right)^2 \right. \\
 & \quad \left. + \left(\frac{\lambda_i \eta^2}{(1 + t\lambda_i \eta)(1 + (t-1)\lambda_i \eta)} \sum_{t'=1}^{t-1} \tilde{u}_i(a, \mathbf{a}_{-i}^{t'}) \right)^2 \right\} \\
 & = \frac{3}{(1 + t\lambda_i \eta)^2} \frac{\exp\{2\eta(\lambda_i \beta_i + 2D_i)\}}{\eta^2(\lambda_i \beta_i + 2D_i)^2} \max_{a \in A_i} \left\{ \left(\frac{\lambda_i \eta}{1 + (t-1)\lambda_i \eta} \log \tau_i(a) \right)^2 + (\eta \tilde{u}_i(a, \mathbf{a}_{-i}^t))^2 \right. \\
 & \quad \left. + \left(\frac{\lambda_i \eta^2}{(1 + (t-1)\lambda_i \eta)} \sum_{t'=1}^{t-1} \tilde{u}_i(a, \mathbf{a}_{-i}^{t'}) \right)^2 \right\} \\
 & \leq \frac{3}{(1 + t\lambda_i \eta)^2} \frac{\exp\{2\eta(\lambda_i \beta_i + 2D_i)\}}{\eta^2(\lambda_i \beta_i + 2D_i)^2} (\lambda^2 \eta^2 \beta_i^2 + 2\eta^2 D_i^2) \\
 & \leq 3 \frac{\exp\{2\eta(\lambda_i \beta_i + 2D_i)\}}{(1 + t\lambda_i \eta)^2} \\
 & \leq 3 \frac{\exp\{2\eta(\lambda_i \beta_i + 2D_i)\}}{(t\lambda_i \eta)^2} = \left(\sqrt{3} \cdot \frac{\exp\{\eta(\lambda_i \beta_i + 2D_i)\}}{t\lambda_i \eta} \right)^2.
 \end{aligned}$$

Using the hypothesis that $\eta \leq 1/(\lambda_i \beta_i + 2D_i)$ and taking square roots yields the statement. \square

A.3. Completing the analysis

Proposition 1. Fix a player $i \in \{1, \dots, n\}$. The regret

$$R_i^T := \max_{\pi^* \in \Delta(A_i)} \sum_{t=1}^T \mathcal{U}_i^t(\pi^*) - \sum_{t=1}^T \mathcal{U}_i^t(\pi_i^t)$$

incurred up to any time T by policies π_i^t defined in (6) where the learning rate is set to any value $0 < \eta \leq 1/(\lambda_i \beta_i + 2D_i)$, satisfies

$$R_i^T \leq \frac{\log |A_i|}{\eta} + \frac{3e(1 + \log T)}{\lambda_i \eta} (D_i + \lambda_i \beta_i + \lambda_i \sqrt{|A_i|}),$$

where D_i is any upper bound on the range of the possible rewards of Player i , and

$$\beta_i := \max_{a \in A_i} \log(1/\tau(a)). \quad (7)$$

Proof. Let

$$\mathbf{q}_i^t := \left(\tilde{u}_i(a, \mathbf{a}_{-i}^t) \right)_{a \in A_i},$$

and note that, by definition of the regularized utilities \mathcal{U}_i ,

$$\begin{aligned}
 \mathcal{U}_i^t(\pi_i^{t+1}) - \mathcal{U}_i^t(\pi_i^t) &= \mathbf{q}_i^\top (\pi_i^{t+1} - \pi_i^t) - \lambda_i D_{\text{KL}}(\pi_i^{t+1} \| \tau) + \lambda_i D_{\text{KL}}(\pi_i^t \| \tau) \\
 &= \mathbf{q}_i^\top (\pi_i^{t+1} - \pi_i^t) - \lambda_i \varphi(\pi_i^{t+1}) + \lambda_i \varphi(\pi_i^t) - \lambda_i \nabla \varphi(\tau_i)^\top (\pi_i^t - \pi_i^{t+1}) \\
 &= (\mathbf{q}_i - \nabla \varphi(\tau_i))^\top (\pi_i^{t+1} - \pi_i^t) - \lambda_i \varphi(\pi_i^{t+1}) + \lambda_i \varphi(\pi_i^t) \\
 &\leq (\mathbf{q}_i + \nabla \varphi(\tau_i))^\top (\pi_i^{t+1} - \pi_i^t) - \lambda_i \varphi(\pi_i^t) - \lambda_i \nabla \varphi(\pi_i^t)^\top (\pi_i^{t+1} - \pi_i^t) + \lambda_i \varphi(\pi_i^t) \\
 &= (\mathbf{q}_i + \lambda_i \nabla \varphi(\tau_i) - \lambda_i \nabla \varphi(\pi_i^t))^\top (\pi_i^{t+1} - \pi_i^t) \\
 &\leq \|\mathbf{q}_i + \lambda_i \nabla \varphi(\tau_i) - \lambda_i \nabla \varphi(\pi_i^t)\|_{\nabla^{-2} \varphi(\pi_i^t)} \cdot \|\pi_i^{t+1} - \pi_i^t\|_{\nabla^2 \varphi(\pi_i^t)},
 \end{aligned}$$

where the first inequality follows by convexity and the second inequality by the generalized Cauchy-Schwarz inequality with the primal-dual norm pair $\|\cdot\|_{\nabla^2 \varphi(\pi_i^t)}$ and $\|\cdot\|_{\nabla^{-2} \varphi(\pi_i^t)}$. A bound for the second term in the product is given by Lemma 4. We now bound the first norm. First,

$$\begin{aligned} \|\mathbf{q}_i + \lambda_i \nabla \varphi(\boldsymbol{\tau}_i) - \lambda_i \nabla \varphi(\pi_i^t)\|_{\nabla^{-2} \varphi(\pi_i^t)}^2 &= \sum_{a \in A_i} \pi_i^t(a) \cdot \left(\tilde{u}_i(a, \mathbf{a}_{-i}^t) + \lambda_i \log \boldsymbol{\tau}_i(a) - \lambda_i \log \pi_i^t(a) \right)^2 \\ &\leq 3 \sum_{a \in A_i} \pi_i^t(a) \cdot \left(\tilde{u}_i(a, \mathbf{a}_{-i}^t)^2 + \lambda_i^2 (\log \boldsymbol{\tau}_i(a))^2 + \lambda_i^2 (\log \pi_i^t(a))^2 \right) \\ &\leq 3(D_i^2 + \lambda_i^2 \beta_i^2 + \lambda_i^2 |A_i|) \\ &\leq 3\left(D_i + \lambda_i \beta_i + \lambda_i \sqrt{|A_i|}\right)^2, \end{aligned}$$

where the second inequality follows from the fact that $x \log^2 x \leq 1$ for all $x \in [0, 1]$. Taking square roots, we find

$$\|\mathbf{q}_i + \lambda_i \nabla \varphi(\boldsymbol{\tau}_i) - \lambda_i \nabla \varphi(\pi_i^t)\|_{\nabla^{-2} \varphi(\pi_i^t)} \leq \sqrt{3} \left(D_i + \lambda_i \beta_i + \lambda_i \sqrt{|A_i|} \right).$$

So, using Lemma 4, we can write

$$\mathcal{U}_i^t(\pi_i^{t+1}) - \mathcal{U}_i^t(\pi_i^t) \leq \frac{3e}{t\lambda_i\eta} (D_i + \lambda_i \beta_i + \lambda_i \sqrt{|A_i|}).$$

Plugging in the above expression into Lemma 1 yields

$$\begin{aligned} R_i^T &\leq \frac{\log |A_i|}{\eta} + \sum_{t=1}^T \frac{3e}{t\lambda_i\eta} (D_i + \lambda_i \beta_i + \lambda_i \sqrt{|A_i|}) \\ &\leq \frac{\log |A_i|}{\eta} + \frac{3e(1 + \log T)}{\lambda_i\eta} (D_i + \lambda_i \beta_i + \lambda_i \sqrt{|A_i|}), \end{aligned}$$

which is the statement. \square

A.4. Proof of Theorem 1

Theorem 1. (*piKL stays close to the anchor policy*) Upon running Algorithm 1 for any T iterations in any multiplayer general-sum game, the average policy $\bar{\pi}_i^T$ of any player i is at a distance

$$D_{\text{KL}}(\bar{\pi}_i^T \parallel \boldsymbol{\tau}_i) \leq \frac{1}{\lambda_i} \left(\frac{R_i^T}{T} + D_i \right).$$

In particular, if $\eta > 0$ is set so that $R_i^T = o(T)$, then $D_{\text{KL}}(\bar{\pi}_i^T \parallel \boldsymbol{\tau}_i) \rightarrow D_i/\lambda_i$ as $T \rightarrow +\infty$.

Proof. By definition of regret,

$$\begin{aligned}
 \frac{1}{T}R_i^T &= \frac{1}{T} \max_{\pi_i^* \in \Delta(A_i)} \left\{ \sum_{t=1}^T \mathcal{U}_i^t(\pi_i^*) - \mathcal{U}_i^t(\pi_i^t) \right\} \\
 &= \max_{\pi_i^* \in \Delta(A_i)} \left\{ \left(\frac{1}{T} \sum_{t=1}^T u_i(\pi_i^*, \pi_{-i}^t) \right) - \left(\frac{1}{T} \sum_{t=1}^T u_i(\pi_i^t, \pi_{-i}^t) \right) - \frac{\lambda_i}{T} \sum_{t=1}^T D_{\text{KL}}(\pi_i^* \parallel \tau_i) + \frac{\lambda_i}{T} \sum_{t=1}^T D_{\text{KL}}(\pi_i^t \parallel \tau_i) \right\} \\
 &= \max_{\pi_i^* \in \Delta(A_i)} \left\{ \left(\frac{1}{T} \sum_{t=1}^T u_i(\pi_i^*, \pi_{-i}^t) \right) - \left(\frac{1}{T} \sum_{t=1}^T u_i(\pi_i^t, \pi_{-i}^t) \right) - \lambda_i D_{\text{KL}}(\pi_i^* \parallel \tau_i) + \frac{\lambda_i}{T} \sum_{t=1}^T D_{\text{KL}}(\pi_i^t \parallel \tau_i) \right\} \\
 &\geq \max_{\pi_i^* \in \Delta(A_i)} \left\{ \left(\frac{1}{T} \sum_{t=1}^T u_i(\pi_i^*, \pi_{-i}^t) \right) - \left(\frac{1}{T} \sum_{t=1}^T u_i(\pi_i^t, \pi_{-i}^t) \right) + \frac{\lambda_i}{T} \sum_{t=1}^T D_{\text{KL}}(\pi_i^t \parallel \tau_i) \right\} \\
 &\geq \max_{\pi_i^* \in \Delta(A_i)} \left\{ \left(\frac{1}{T} \sum_{t=1}^T u_i(\pi_i^*, \pi_{-i}^t) \right) - \left(\frac{1}{T} \sum_{t=1}^T u_i(\pi_i^t, \pi_{-i}^t) \right) + \lambda_i D_{\text{KL}}(\bar{\pi}_i^T \parallel \tau_i) \right\} \\
 &= \max_{\pi_i^* \in \Delta(A_i)} \left\{ \left(\frac{1}{T} \sum_{t=1}^T (u_i(\pi_i^*, \pi_{-i}^t) - u_i(\pi_i^t, \pi_{-i}^t)) \right) + \lambda_i D_{\text{KL}}(\bar{\pi}_i^T \parallel \tau_i) \right\} \\
 &\geq \max_{\pi_i^* \in \Delta(A_i)} \left\{ \left(\frac{1}{T} \sum_{t=1}^T -D_i \right) + \lambda_i D_{\text{KL}}(\bar{\pi}_i^T \parallel \tau_i) \right\} = -D_i + \lambda_i D_{\text{KL}}(\bar{\pi}_i^T \parallel \tau_i),
 \end{aligned}$$

where the first inequality holds since the KL divergence is nonnegative, the second inequality by convexity of the KL divergence, and the third inequality by definition of D_i . Rearranging yields the inequality in the statement. \square

A.5. Relationship with Nash Equilibrium

In this subsection, we show that when all players play according to Algorithm 1 in a *two-player zero-sum* game, then the average policies $\bar{\pi}_i^T$ converge to a Nash equilibrium of the regularized game whose utilities are \mathcal{U}_i .

Proposition 2. For any $T \in \mathbb{N}$, $\eta > 0$, and $\delta \in (0, 1)$, define the quantity

$$\xi^T(\delta) := \frac{R_1^T + R_2^T}{T} + D_i \sqrt{\frac{32}{T} \log \frac{2}{\delta}}.$$

Upon running Algorithm 1 for any T iterations with learning rate $\eta > 0$, the average policies $\bar{\pi}_i^T$ of each player form a $\xi^T(\delta)$ -approximate Nash equilibrium with respect to the regularized utility functions \mathcal{U}_i with probability at least $1 - \delta$, for any $\delta \in (0, 1)$.

Proof. Fix a player $i \in \{1, 2\}$, and any policy $\pi^* \in \Delta(A_i)$, and introduce the discrete-time stochastic process

$$w^t := \left(\mathcal{U}_i(\pi^*, \pi_{-i}^t) - \mathcal{U}_i(\pi_i^t, \pi_{-i}^t) \right) - \left(\mathcal{U}_i(\pi^*, a_{-i}^t) - \mathcal{U}_i(\pi_i^t, a_{-i}^t) \right).$$

Since the opponent player $-i$ plays according to Algorithm 1, its action a_{-i}^t at all times t is selected by sampling (unbiasedly) an action from the policy π_{-i}^t . Therefore, w^t is a martingale difference sequence. Furthermore, by expanding the definition of \mathcal{U}_i , the absolute value of w^t satisfies

$$\begin{aligned}
 |w^t| &= \left| \left(u_i(\pi^*, \pi_{-i}^t) - u_i(\pi_i^t, \pi_{-i}^t) \right) - \left(u_i(\pi^*, a_{-i}^t) - u_i(\pi_i^t, a_{-i}^t) \right) \right| \\
 &\leq \left| u_i(\pi^*, \pi_{-i}^t) - u_i(\pi_i^t, \pi_{-i}^t) \right| + \left| u_i(\pi^*, a_{-i}^t) - u_i(\pi_i^t, a_{-i}^t) \right| \leq 2D_i.
 \end{aligned}$$

Hence, using Azuma-Hoeffding's inequality, for any $\delta \in (0, 1)$,

$$\begin{aligned}
 1 - \delta &\leq \mathbb{P} \left[\sum_{t=1}^T w^t \leq D_i \sqrt{8T \log \frac{1}{\delta}} \right] \\
 &= \mathbb{P} \left[\left(\sum_{t=1}^T \mathcal{U}_i(\pi^*, \pi_{-i}^t) - \sum_{t=1}^T \mathcal{U}_i(\pi_i^t, \pi_{-i}^t) \right) - \left(\sum_{t=1}^T u_i(\pi^*, a_{-i}^t) - \sum_{t=1}^T \mathcal{U}_i(\pi_i^t, a_{-i}^t) \right) \leq \sqrt{8T \log \frac{1}{\delta}} \right] \\
 &= \mathbb{P} \left[\sum_{t=1}^T \mathcal{U}_i(\pi^*, \pi_{-i}^t) - \sum_{t=1}^T \mathcal{U}_i(\pi_i^t, \pi_{-i}^t) \leq R_i^T + D_i \sqrt{8T \log \frac{1}{\delta}} \right],
 \end{aligned}$$

where R_i^T is as defined in Proposition 1. Since the above expression holds for any $\pi^* \in \Delta(A_i)$, in particular,

$$\mathbb{P} \left[\max_{\pi^* \in \Delta(A_i)} \sum_{t=1}^T \mathcal{U}_i(\pi^*, \pi_{-i}^t) - \sum_{t=1}^T \mathcal{U}_i(\pi_i^t, \pi_{-i}^t) \leq R_i^T + D_i \sqrt{8T \log \frac{1}{\delta}} \right] \geq 1 - \delta \quad (22)$$

for any player $i \in \{1, 2\}$ and any $\delta \in (0, 1)$.

Summing Inequality (22) for $i \in \{1, 2\}$ and using the union bound, we can further write

$$\begin{aligned}
 \mathbb{P} \left[\max_{\pi_1^* \in \Delta(A_1)} \left\{ \sum_{t=1}^T \mathcal{U}_1(\pi_1^*, \pi_2^t) \right\} + \max_{\pi_2^* \in \Delta(A_2)} \left\{ \sum_{t=1}^T \mathcal{U}_2(\pi_1^t, \pi_2^*) \right\} - \left(\sum_{t=1}^T \mathcal{U}_1(\pi_1^t, \pi_2^t) + \mathcal{U}_2(\pi_1^t, \pi_2^t) \right) \right. \\
 \left. \leq R_1^T + R_2^T + D_i \sqrt{32T \log \frac{1}{\delta}} \right] \geq 1 - 2\delta.
 \end{aligned}$$

Dividing by T and noting that for any player $i \in \{1, 2\}$

$$\frac{1}{T} \sum_{t=1}^T \mathcal{U}_i(\pi^*, \pi_{-i}^t) = \mathcal{U}_i \left(\pi^*, \frac{1}{T} \sum_{t=1}^T \pi_{-i}^t \right) = \mathcal{U}_i(\pi^*, \bar{\pi}_{-i}^T)$$

further yields

$$\begin{aligned}
 \mathbb{P} \left[\max_{\pi_1^* \in \Delta(A_1)} \{ \mathcal{U}_1(\pi_1^*, \bar{\pi}_2^T) \} + \max_{\pi_2^* \in \Delta(A_2)} \{ \mathcal{U}_2(\bar{\pi}_1^T, \pi_2^*) \} - \frac{1}{T} \left(\sum_{t=1}^T \mathcal{U}_1(\pi_1^t, \pi_2^t) + \mathcal{U}_2(\pi_1^t, \pi_2^t) \right) \right. \\
 \left. \leq \frac{R_1^T + R_2^T}{T} + D_i \sqrt{\frac{32}{T} \log \frac{1}{\delta}} \right] \geq 1 - 2\delta. \quad (23)
 \end{aligned}$$

We now analyze the term in parenthesis, that is,

$$(\clubsuit) := -\frac{1}{T} \left(\sum_{t=1}^T \mathcal{U}_1(\pi_1^t, \pi_2^t) + \mathcal{U}_2(\pi_1^t, \pi_2^t) \right)$$

Plugging in the definition of \mathcal{U}_1 and \mathcal{U}_2 , that is,

$$\begin{aligned}
 \mathcal{U}_1(\pi_1, \pi_2) &:= u_1(\pi_1, \pi_2) - \lambda_1 D_{\text{KL}}(\pi_1 \| \tau_1) \\
 \mathcal{U}_2(\pi_1, \pi_2) &:= u_2(\pi_1, \pi_2) - \lambda_2 D_{\text{KL}}(\pi_2 \| \tau_2) = -u_1(\pi_1, \pi_2) + \lambda_2 D_{\text{KL}}(\pi_2 \| \tau_2)
 \end{aligned}$$

into (\clubsuit) yields

$$\begin{aligned}
 (\clubsuit) &= -\frac{1}{T} \left(\sum_{t=1}^T \mathcal{U}_1(\pi_1^t, \pi_2^t) + \mathcal{U}_2(\pi_1^t, \pi_2^t) \right) = \frac{1}{T} \left(\sum_{t=1}^T \lambda_1 D_{\text{KL}}(\pi_1^t \| \tau_1) + \lambda_2 D_{\text{KL}}(\pi_2^t \| \tau_2) \right) \\
 &\geq \lambda_1 D_{\text{KL}}(\bar{\pi}_1^T \| \tau_1) + \lambda_2 D_{\text{KL}}(\bar{\pi}_2^T \| \tau_2) \quad (24) \\
 &= -(\mathcal{U}_1(\bar{\pi}_1^T, \bar{\pi}_2^T) + \mathcal{U}_2(\bar{\pi}_1^T, \bar{\pi}_2^T)), \quad (25)
 \end{aligned}$$

where (24) follows from convexity of the KL divergence function, and (25) follows again from the definition of \mathcal{U}_1 and \mathcal{U}_2 . Substituting (25) back into (23), we find

$$\begin{aligned} \mathbb{P} \left[\max_{\pi_1^* \in \Delta(A_1)} \{ \mathcal{U}_1(\pi_1^*, \bar{\pi}_2^T) - \mathcal{U}_1(\bar{\pi}_1^T, \bar{\pi}_2^T) \} + \max_{\pi_2^* \in \Delta(A_2)} \{ \mathcal{U}_2(\bar{\pi}_1^T, \pi_2^*) - \mathcal{U}_2(\bar{\pi}_1^T, \bar{\pi}_2^T) \} \right. \\ \left. \leq \frac{R_1^T + R_2^T}{T} + D_i \sqrt{\frac{32}{T} \log \frac{1}{\delta}} \right] \geq 1 - 2\delta. \quad (26) \end{aligned}$$

Since

$$\max_{\pi_1^* \in \Delta(A_1)} \{ \mathcal{U}_1(\pi_1^*, \bar{\pi}_2^T) - \mathcal{U}_1(\bar{\pi}_1^T, \bar{\pi}_2^T) \} \geq 0, \quad \text{and} \quad \max_{\pi_2^* \in \Delta(A_2)} \{ \mathcal{U}_2(\bar{\pi}_1^T, \pi_2^*) - \mathcal{U}_2(\bar{\pi}_1^T, \bar{\pi}_2^T) \} \geq 0,$$

the inequality above in particular implies that

$$\begin{aligned} \mathbb{P} \left[\max \left\{ \max_{\pi_1^* \in \Delta(A_1)} \{ \mathcal{U}_1(\pi_1^*, \bar{\pi}_2^T) - \mathcal{U}_1(\bar{\pi}_1^T, \bar{\pi}_2^T) \}, \max_{\pi_2^* \in \Delta(A_2)} \{ \mathcal{U}_2(\bar{\pi}_1^T, \pi_2^*) - \mathcal{U}_2(\bar{\pi}_1^T, \bar{\pi}_2^T) \} \right\} \right. \\ \left. \leq \frac{R_1^T + R_2^T}{T} + D_i \sqrt{\frac{32}{T} \log \frac{1}{\delta}} \right] \geq 1 - 2\delta, \quad (27) \end{aligned}$$

which is equivalent to the statement after making the variable substitution $\delta := \delta'/2$. \square

In particular, when $\eta \leq 1/(\lambda_i \beta_i + 2D_i)$ for both players $i \in \{1, 2\}$, Proposition 2 implies that the average strategy profile is a $O(1/\sqrt{T})$ -Nash equilibrium with respect to the regularized utility functions \mathcal{U}_i .

A standard application of the Borel-Cantelli lemma enables to convert from the high-proability guarantees of Proposition 2 at finite time to almost-sure convergence in the limit. Specifically,

Corollary 1. *Let $(\bar{\pi}_1, \bar{\pi}_2)$ be any limit point of the average policies $(\bar{\pi}_1^T, \bar{\pi}_2^T)$ of the players. Almost surely, $(\bar{\pi}_1, \bar{\pi}_2)$ is a Nash equilibrium with respect to the regularized utility functions $\mathcal{U}_1, \mathcal{U}_2$, respectively.*

From there, it is immediate to give guarantees with respect to the original (i.e., unregularized) game, and Theorem 2 follows.

Theorem 2. *Let $(\bar{\pi}_1, \bar{\pi}_2)$ be any limit point of the average policies $(\bar{\pi}_1^T, \bar{\pi}_2^T)$ of the players. Almost surely, $(\bar{\pi}_1, \bar{\pi}_2)$ is a $(\max_{i=1,2} \{\lambda_i \beta_i\})$ -approximate Nash equilibrium policy with respect to the original utility functions u_i , where β_i is as defined in (7).*

Proof. From Corollary 1, almost surely $(\bar{\pi}_1, \bar{\pi}_2)$ is a Nash equilibrium of the regularized game whose players' utilities are \mathcal{U}_1 and \mathcal{U}_2 , respectively. Expanding the definition of Nash equilibrium relative to Player 1, we have that

$$\begin{aligned} 0 &= \max_{\pi_1^* \in \Delta(A_1)} \{ \mathcal{U}_1(\pi_1^*, \bar{\pi}_2) - \mathcal{U}_1(\bar{\pi}_1, \bar{\pi}_2) \} \\ &= \max_{\pi_1^* \in \Delta(A_1)} \{ u_1(\pi_1^*, \bar{\pi}_2) - \lambda_1 D_{\text{KL}}(\pi_1^* \parallel \tau_1) - u_1(\bar{\pi}_1, \bar{\pi}_2) + \lambda_1 D_{\text{KL}}(\bar{\pi}_1 \parallel \tau_1) \} \\ &\geq \max_{\pi_1^* \in \Delta(A_1)} \{ u_1(\pi_1^*, \bar{\pi}_2) - u_1(\bar{\pi}_1, \bar{\pi}_2) \} - \lambda_1 D_{\text{KL}}(\pi_1^* \parallel \tau_1) \\ &= \max_{\pi_1^* \in \Delta(A_1)} \left\{ (u_1(\pi_1^*, \bar{\pi}_2) - u_1(\bar{\pi}_1, \bar{\pi}_2)) - \lambda_1 \sum_{a \in A_1} \pi_1^*(a) \log(\pi_1^*(a)) - \lambda_1 \sum_{a \in A_1} \pi_1^*(a) \log(1/\tau_1(a)) \right\} \\ &\geq \max_{\pi_1^* \in \Delta(A_1)} \left\{ (u_1(\pi_1^*, \bar{\pi}_2) - u_1(\bar{\pi}_1, \bar{\pi}_2)) - \lambda_1 \sum_{a \in A_1} \pi_1^*(a) \log(1/\tau_1(a)) \right\} \\ &\geq \max_{\pi_1^* \in \Delta(A_1)} \{ u_1(\pi_1^*, \bar{\pi}_2) - u_1(\bar{\pi}_1, \bar{\pi}_2) \} - \lambda_1 \beta_1, \end{aligned}$$

where the first inequality follows since the KL divergence is always nonnegative, the second inequality since the negative entropy function is nonpositive on the simplex, and the third inequality follows from the definition of β_1 . Symmetrically, for Player 2 we find that

$$0 \geq \max_{\pi_2^* \in \Delta(A_2)} \{u_2(\bar{\pi}_1, \pi_2^*) - u_2(\bar{\pi}_1, \bar{\pi}_2)\} - \lambda_2 \beta_2.$$

Hence, the exploitability of $\bar{\pi}_1$ is at most $\lambda_1 \beta_1$, while the exploitability of $\bar{\pi}_2$ is at most $\lambda_2 \beta_2$, which immediately implies the statement. \square

B. Illustrations of piKL-Hedge in Blotto

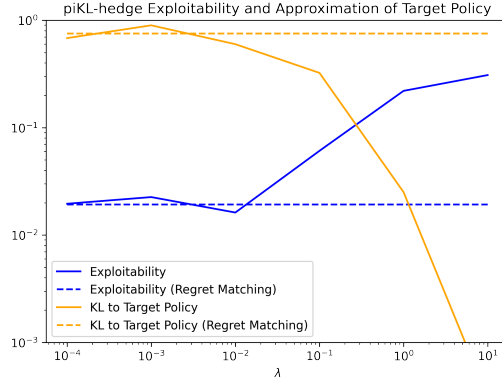


Figure 6. Comparison of piKL and regret matching as a function of λ in Colonel Blotto(10, 3). As λ increases in piKL-hedge, piKL moves closer to the anchor policy at the cost of increased exploitability. The scale of λ is related to the scale of the payoffs in the game, which are $[0, 1]$ in Blotto.

Colonel Blotto is a famous 2-player simultaneous action game that has a large action space but has rules that are short and simple. In Blotto, each player has c coins to be distributed across f fields. The aim is to win the most fields by allocating the player’s coins across the fields. A field is won by contributing the most coins to that field (and drawn if there is a tie). The winner receives a reward of +1 and the loser receives -1. Both receive 0 in the case of a tie.

In Figure 6 we illustrate the key features of piKL-Hedge in Blotto, using a uniform anchor policy for convenience. Incidentally, piKL-Hedge with a uniform anchor policy converges to a quantal response equilibrium (McKelvey & Palfrey, 1995b). piKL-Hedge finds policies that play close to the anchor policy while having low regret, with λ controlling the relative optimality of these two desiderata.

C. Human Policy KL-Regularized Search also improves Cross-Entropy

| Model | Dataset | (raw model) | $c_{\text{puct}} = 10$ | $c_{\text{puct}} = 5$ | $c_{\text{puct}} = 2$ | $c_{\text{puct}} = 1$ | $c_{\text{puct}} = 0.5$ |
|------------------|----------------------------|-------------|------------------------|-----------------------|-----------------------|-----------------------|-------------------------|
| Maia1500 (Chess) | Lichess 1500 Rating Bucket | 1.473 | 1.466 | 1.462 | 1.467 | 1.502 | 1.596 |
| Maia1900 (Chess) | Lichess 1900 Rating Bucket | 1.440 | 1.429 | 1.422 | 1.418 | 1.444 | 1.530 |
| Our Model (Go) | GoGoD | 1.388 | 1.362 | 1.359 | 1.362 | 1.391 | 1.478 |

Table 5. Cross-entropy predicting human moves in chess and Go using smooth KL optimization post-processing of MCTS with various c_{puct} .

Here we show that not only does policy-regularized search improve top-1 accuracy, it also improves cross entropy for a reasonable range of parameter values in both chess and Go.

To obtain the policy distribution with which to compute its cross entropy with the human data, unlike for top-1 accuracy or for play we cannot directly use the MCTS visit distribution because occasionally simply due to discretization MCTS may give zero visits to the actual move that a human played, resulting in an undefined (i.e. infinite) cross-entropy. Instead, we leverage the result of Grill et al. (2020) that PUCT-style MCTS with a policy prior can be seen as a discrete approximation

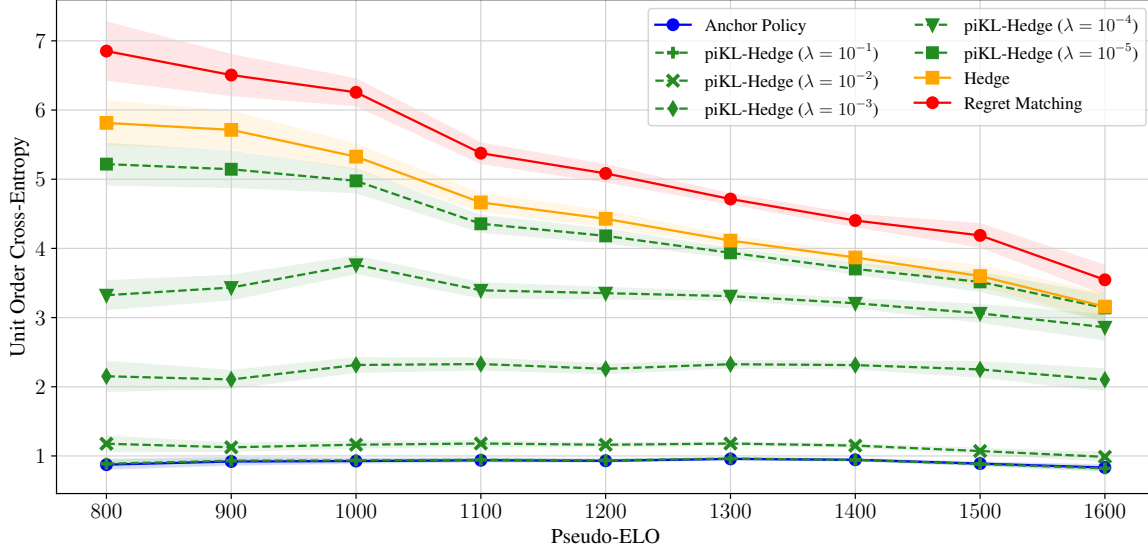


Figure 7. Average cross-entropy of per-unit order prediction in Diplomacy, comparing the human-imitation-learned anchor policy, regret matching, hedge, and piKL-Hedge, as a function of pseudo-Elo player rating.

to solving a smooth optimization:

$$\arg \max_{\pi} \sum_a Q(s, a) \pi(s, a) + \lambda D_{\text{KL}}(\tau \parallel \pi)$$

where

$$\lambda = c_{\text{puct}} \frac{\sqrt{\sum_a n_a}}{(k + \sum_a n_a)}$$

where, q is the vector of Q-values of moves, τ is the anchor or prior policy, λ controls the strength of the regularization towards that prior as a function of the number of visits, c_{puct} is the MCTS exploration coefficient, and k is an arbitrary constant not affecting the asymptotic results.

We perform MCTS exactly the same as normal, the only difference is that at the very end, rather than using visit counts, we compute π optimizing the above objective using the human imitation-learned anchor policy for τ and the MCTS-estimated Q-values for Q (and using the same unweighted average child value for moves that lack a Q-value estimate due to having zero visits as described in Appendix I). We use this resulting smooth π as the final policy prediction and compute its cross entropy with the actual human moves.

Note that the authors choose $k = |A|$, the number of legal actions, for mathematical convenience, corresponding to adding one extra visit per every possible action (Grill et al., 2020), but since in our experiments we use only use 50 visits including the root visit (i.e. $\sum_a n_a = 49$), and the branching factor can be as large as 362 in Go, adding one extra visit per legal action in our case greatly overestimates the total number of visits, which in practice gives a less accurate correspondence between MCTS and this smoother regularized solution, so we instead choose $k = 0$.

In Table 5 we show the results. Across roughly the same parameter ranges, the regularized search policy using this smoothed MCTS postprocessing achieves lower cross-entropy with human moves than the raw imitation-learned policy without search. This suggests that not only does search improve on the raw imitation-learned policy at pinpointing the top action, it also gives a more accurate model of the overall distribution of likely human actions.

Similarly, in Figure 7, we show that piKL-Hedge achieves better average cross entropy of unit orders in Diplomacy compared to unregularized search methods. This further implies that piKL-Hedge not only does better at predicting the top action but that it also better models the overall distribution of human actions better.

D. Diplomacy hyper-parameters

We describe the search parameters used in this work and compare it to those in previous works. As compared to Gray et al. (2020), we use a much less expensive set of search parameters for all results in the main section of this paper Table 7. In Table 8, we show that these tuned-down set of parameters, slightly reduces piKL-HedgeBot’s performance but allows us to make similar conclusions when comparing against SearchBot (Gray et al., 2020) and supervised learning bots from prior works. Additionally, in Table 8, we also show that when our agent (piKL-HedgeBot ($\lambda = 0.001$)) uses the same search parameters as Gray et al. (2020), it outperforms SearchBot by a big margin.

In our experiments, to compare against DipNet (Paquette et al., 2019) we use the original model checkpoint⁶ and we sample from the policy with temperature 0.1 (as used in prior works). Similarly, to compare against SearchBot (Gray et al., 2020) agent we use the released checkpoint⁷ and agent configuration⁸.

The only other search parameter unique and new to our piKL-HedgeBot algorithm is η in Algorithm 1, which we heuristically set on each Hedge iteration t to $c/(\sigma\sqrt{t})$ where σ is the standard deviation across iterations of the average utility experienced by the agent i being updated. We find $c = 10/3$ works well for no-press Diplomacy.

| Model | Temperature |
|-----------------------------------|-------------|
| DipNet (Paquette et al., 2019) | 0.1 |
| DipNet RL (Paquette et al., 2019) | 0.1 |
| Blueprint (Gray et al., 2020) | 0.1 |
| SL Policy (Ours) | 0.5 |

Table 6. Sampling temperatures used in the supervised learning models across prior works. For our supervised learning model (SL Policy), we use a temperature of 0.5 in all experiments to encourage stochasticity.

| Parameter | (Gray et al., 2020) | Ours |
|--|---------------------|------|
| Number candidate actions (N_c) | 50 | 30 |
| Max candidate actions per unit | 3.5 | 3.5 |
| Number search iterations | 256 | 512 |
| Policy sampling temperature for rollouts | 0.75 | N/A |
| Policy sampling top-p | 0.95 | 0.95 |
| Rollout length, move phases | 2 | 0 |

Table 7. Search parameters used in Gray et al. (2020) compared to the search parameters used in our work. All experiments in the main body of this work uses search settings that are much cheaper to run. We use a rollout length of 0 and $N_c = 30$ while increasing the number of search iterations to 512.

| 1x \downarrow 6x \rightarrow | DipNet | DipNet RL | Blueprint | BRBot | SearchBot |
|--|------------------|------------------|------------------|------------------|------------------|
| DipNet (Paquette et al., 2019) | - | 6.7% \pm 0.9% | 11.6% \pm 0.1% | 0.1% \pm 0.1% | 0.7% \pm 0.2% |
| DipNet RL (Paquette et al., 2019) | 18.9% \pm 1.4% | - | 10.5% \pm 1.1% | 0.1% \pm 0.1% | 0.6% \pm 0.2% |
| Blueprint (Gray et al., 2020) | 20.2% \pm 1.3% | 7.5% \pm 1.0% | - | 0.3% \pm 0.1% | 0.9% \pm 0.2% |
| BRBot (Gray et al., 2020) | 67.3% \pm 1.0% | 43.7% \pm 1.0% | 69.3% \pm 1.7% | - | 11.1% \pm 1.1% |
| SearchBot (Gray et al., 2020) | 51.1% \pm 1.9% | 35.2% \pm 1.8% | 52.7% \pm 1.3% | 17.2% \pm 1.3% | - |
| piKL-HedgeBot ($\lambda = 0.001$) | 54.8% \pm 1.8% | 31.4% \pm 1.8% | 50.3% \pm 1.8% | 19.2% \pm 1.4% | 16.6% \pm 1.3% |
| piKL-HedgeBot ($\lambda = 0.001$) ((Gray et al., 2020) parameters) | 60.1% \pm 1.8% | 33.3% \pm 1.8% | 58.1% \pm 1.8% | 23.6% \pm 1.6% | 20.3% \pm 1.4% |

Table 8. Average SoS scores achieved by the 1x agent against the 6x agents. This table compares the performance of SearchBot (Gray et al., 2020) and other agents from prior work with piKL-HedgeBot ($\lambda = 0.001$) that uses a much cheaper search setting. Using the much cheaper search setting, comes at relatively small cost in its performance as we use improved value and policy models (See, Appendix E and Appendix D for more details). When using the same parameters as Gray et al. (2020), piKL-HedgeBot ($\lambda = 0.001$) significantly outperforms SearchBot under most settings. Note that equal performance would be $1/7 \approx 14.3\%$. The \pm shows one standard error.

⁶DipNet SL from <https://github.com/diplomacy/research>.

⁷blueprint from https://github.com/facebookresearch/diplomacy_searchbot/releases/tag/1.0.

⁸https://github.com/facebookresearch/diplomacy_searchbot/blob/master/conf/common/agents/searchbot_02_fastbot.prototxt

E. Diplomacy Model Architecture and Input Features

Our supervised learning policy model for Diplomacy uses the same transformer-encoder LSTM-decoder architecture as Bakhtin et al. (2021) for reinforcement learning in Diplomacy, but applied to imitation learning over human games. This architecture also resembles the architecture used by a significant amount of past work (Gray et al., 2020; Anthony et al., 2020; Paquette et al., 2019) but replaces the graph-convolution encoder with a transformer, which we find to produce good results.

Additionally, we slightly modify the input feature encoding relative to Gray et al. (2020), removing a small number of redundant channels and adding channels to indicate the “home centers” of each of the 7 powers (Austria, England, France,... etc), which are the locations where that power is allowed to build new armies or fleets. See Table 9 for the new list of input features. By adding the home centers to the input encoding instead of leaving them implicit, the game becomes entirely equivariant to permutations of those powers - e.g. if one swaps all the units of England and France, and all their centers, and which centers are their home centers, the resulting game is isomorphic to the original except with the two powers renamed.

This allows us to then augment the training data via equivariant permutations of the seven possible powers in the encoding. Every time we sample a position from the dataset for training, we also choose among all 7-factorial permutations of the powers uniformly at random, and correspondingly permute both the input and output, to reduce overfit and improve the model’s generalization given the limited human data available.

| Feature | Type | Number of Channels |
|------------------------------|--|--------------------|
| Location has unit? | One-hot (army/fleet), or all zero | 2 |
| Owner of unit | One-hot (7 powers), or all zero | 7 |
| Buildable, Removable? | Binary | 2 |
| Location has dislodged unit? | One-hot (army/fleet), or all zero | 2 |
| Owner of dislodged unit | One-hot (7 powers), or all zero | 7 |
| Area type | One-hot (land,coast,water) | 3 |
| Supply center owner | One-hot (7 powers or neutral), or all zero | 8 |
| Home center | One-hot (7 powers), or all zero | 7 |

Table 9. Per-location input features used

F. Improved Value Model in Diplomacy

For no-press Diplomacy, we note that Gray et al. (2020) observed that their search agent benefits from short rollouts using the trained human policy before applying the human-learned value model to evaluate the position. Doing so appears to result in more accurate evaluations reflecting the likely outcomes from a given game state, which the raw value model may failed to learn sufficiently accurately on the limited human dataset. Since expectation of the learned value model after a short rollout appears to be better than the learned value model itself, this motivates training a model to directly approximate the former.

In a fashion broadly similar to Silver et al. (2016) generating rollout games to train a more accurate value head for Go, we therefore generated a large stream of data by uniformly sampling positions from the human game dataset for Diplomacy, rolling them forward between 4-8 phases of game play via the same rollout settings as Gray et al. (2020), i.e. policy sampling temperature 0.75, top-p 0.95, and training a new value head to predict the resulting post-rollout value estimate of the old value model. Samples were continuously and asynchronously added to a replay buffer of 10000 batches, and the buffer was continuously sampled to train the same transformer-based architecture as the human-trained model from Appendix E initialized with the weights of that model. Training was constrained to never exceed the rate of data generation by more than a factor of 2 (i.e. using each sample twice in expectation) and proceeded for 128000 mini-batches of 1024 samples each using the ADAM optimizer with a fixed learning rate of $1e-5$.

G. More Experiments in Diplomacy

This section compiles additional performance results from evaluation games.

G.1. Head-to-Head Performance

In Table 10, we compare the performance of piKL-HedgeBot in 1v6 head-to-head games against the underlying supervised anchor policy, following prior work (Gray et al., 2020; Bakhtin et al., 2021; Paquette et al., 2019; Anthony et al., 2020). We find that the $\lambda = 0.1$ policy is substantially stronger than the supervised policy while matching the accuracy in predicting human moves, while the $\lambda=1e-3$ policy outperforms unregularized search methods while playing much closer to the human policy.

| 1x | 6x | Average SoS Score | 1x | 6x | Average SoS Score |
|-----------|-----------------------------------|-------------------|-----------|-----------------------------------|-------------------|
| SL Policy | piKL-HedgeBot($\lambda = 1e-1$) | $8.3 \pm 0.9\%$ | SL Policy | piKL-HedgeBot($\lambda = 1e-1$) | $21.1 \pm 1.4\%$ |
| | piKL-HedgeBot($\lambda = 1e-2$) | $2.5 \pm 0.4\%$ | | piKL-HedgeBot($\lambda = 1e-2$) | $44.2 \pm 1.7\%$ |
| | piKL-HedgeBot($\lambda = 1e-3$) | $1.8 \pm 0.3\%$ | | piKL-HedgeBot($\lambda = 1e-3$) | $52.7 \pm 1.7\%$ |
| | piKL-HedgeBot($\lambda = 1e-4$) | $2.1 \pm 0.3\%$ | | piKL-HedgeBot($\lambda = 1e-4$) | $49.7 \pm 1.7\%$ |
| | piKL-HedgeBot($\lambda = 1e-5$) | $1.6 \pm 0.2\%$ | | piKL-HedgeBot($\lambda = 1e-5$) | $46.9 \pm 1.7\%$ |
| | HedgeBot | $1.5 \pm 0.2\%$ | | HedgeBot | $46.5 \pm 1.7\%$ |
| | RMBot | $1.4 \pm 0.2\%$ | | RMBot | $46.2 \pm 1.7\%$ |

Table 10. Average SoS score attained by the 1x agent against the 6x agent. piKL-HedgeBot($\lambda = 0.1$) policy is substantially stronger than SL Policy, while the ($\lambda = 0.01$) policy is almost as strong as RMBot. The \pm shows one standard error. Note that equal performance would be $1/7 \approx 14.3\%$.

G.2. piKL-HedgeBot’s performance in population-based experiments

In this section, we provide all the results from the population experiments across various piKL-HedgeBot’s lambda values. Figure 8 and Table 11 show the results. piKL-HedgeBot with $\lambda=1e-3$ performs best across individual population experiments with an SoS score of 32.9%. The performance drops as we continue to increase λ past $1e-3$. Error bars indicate 1 standard error.

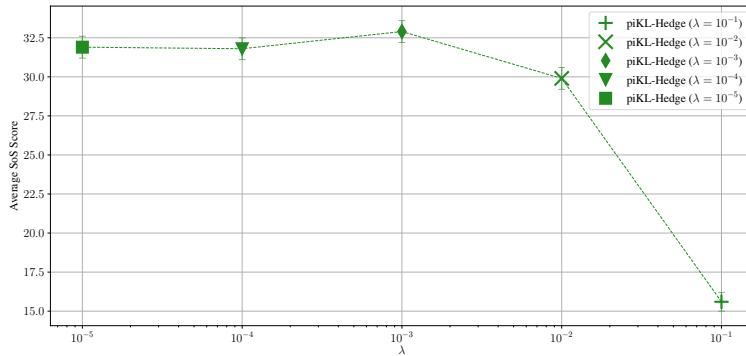


Figure 8. Average SoS score achieved by piKL-HedgeBots in uniformly sampled pools of other agents as a function of λ . piKL-HedgeBot ($\lambda = 10^{-3}$) performs best across individual sweeps with an SoS score of 32.9%.

| Agent | Average SoS Score | Agent | Average SoS Score |
|-----------------------------------|-------------------|-----------------------------------|-------------------|
| DipNet (Paquette et al., 2019) | 4.9% \pm 0.3% | DipNet (Paquette et al., 2019) | 3.8% \pm 0.3% |
| DipNet RL (Paquette et al., 2019) | 5.6% \pm 0.4% | DipNet RL (Paquette et al., 2019) | 4.2% \pm 0.3% |
| Blueprint (Gray et al., 2020) | 7.1% \pm 0.4% | Blueprint (Gray et al., 2020) | 5.8% \pm 0.4% |
| BRBot (Gray et al., 2020) | 18.2% \pm 0.6% | BRBot (Gray et al., 2020) | 16.3% \pm 0.6% |
| SearchBot (Gray et al., 2020) | 36.1% \pm 0.8% | SearchBot (Gray et al., 2020) | 14.1% \pm 0.6% |
| SL Policy | 10.2% \pm 0.6% | SL Policy | 8.5% \pm 0.4% |
| RMBot | 36.8% \pm 1.1% | RMBot | 31.7% \pm 0.8% |
| piKL-HedgeBot($\lambda = 1e-1$) | 15.6% \pm 0.6% | piKL-HedgeBot($\lambda = 1e-2$) | 29.9% \pm 0.7% |
| Agent | Average SoS Score | Agent | Average SoS Score |
| DipNet (Paquette et al., 2019) | 3.7% \pm 0.3% | DipNet (Paquette et al., 2019) | 3.5% \pm 0.3% |
| DipNet RL (Paquette et al., 2019) | 4.7% \pm 0.3% | DipNet RL (Paquette et al., 2019) | 4.6% \pm 0.3% |
| Blueprint (Gray et al., 2020) | 4.9% \pm 0.3% | Blueprint (Gray et al., 2020) | 5.7% \pm 0.3% |
| BRBot (Gray et al., 2020) | 16.1% \pm 0.6% | BRBot (Gray et al., 2020) | 14.3% \pm 0.6% |
| SearchBot (Gray et al., 2020) | 13.4% \pm 0.5% | SearchBot (Gray et al., 2020) | 13.6% \pm 0.5% |
| SL Policy | 7.9% \pm 0.4% | SL Policy | 8.8% \pm 0.4% |
| RMBot | 31.3% \pm 0.7% | RMBot | 31.8% \pm 0.7% |
| piKL-HedgeBot($\lambda = 1e-3$) | 32.9% \pm 0.7% | piKL-HedgeBot($\lambda = 1e-4$) | 31.8% \pm 0.7% |
| Agent | Average SoS Score | Agent | Average SoS Score |
| DipNet (Paquette et al., 2019) | 3.6% \pm 0.3% | DipNet (Paquette et al., 2019) | 3.6% \pm 0.3% |
| DipNet RL (Paquette et al., 2019) | 4.4% \pm 0.3% | DipNet RL (Paquette et al., 2019) | 3.9% \pm 0.3% |
| Blueprint (Gray et al., 2020) | 5.3% \pm 0.3% | Blueprint (Gray et al., 2020) | 5.5% \pm 0.3% |
| BRBot (Gray et al., 2020) | 15.0% \pm 0.6% | BRBot (Gray et al., 2020) | 14.7% \pm 0.6% |
| SearchBot (Gray et al., 2020) | 13.0% \pm 0.5% | SearchBot (Gray et al., 2020) | 14.1% \pm 0.6% |
| SL Policy | 8.9% \pm 0.4% | SL Policy | 8.7% \pm 0.4% |
| RMBot | 32.2% \pm 0.7% | RMBot | 32.2% \pm 0.7% |
| piKL-HedgeBot($\lambda = 1e-5$) | 31.9% \pm 0.7% | HedgeBot | 31.7% \pm 0.7% |

Table 11. Average SoS score achieved by agents in uniformly sampled pools of other agents. piKL-HedgeBot with $\lambda=1e-3$ performs best across individual sweeps with an SoS score of 32.9%. The \pm shows one standard error.

H. Baseline Model Architecture and Training for Go

As summarized in Section 3.2.1, for training baseline imitation-learning models to play on the 19x19 board in Go, our architecture follows the same 20-block 256-channel residual net described in Silver et al. (2017), except with the addition of squeeze-and-excitation layers at the end of each residual block (Hu et al., 2018). In particular, the following additional operations are inserted just prior to each skip connection that adds the output R of a residual block to the trunk X :

- Channelwise global average pooling of R from $19 \times 19 \times 256$ channels to 256 channels.
- A fully connected layer including bias from 256 channels to 64 channels.
- A ReLU nonlinearity.
- A fully connected layer including bias from 64 channels to 512 channels, which are split two vectors S and B of 256 channels each.
- Output $R \times \text{sigmoid}(S) + B$ to be added back to the trunk X , instead of R as in a normal residual net.

In other words, the final result of the residual block as a whole is $\text{ReLU}(X + R \times \text{sigmoid}(S) + B)$ instead of $\text{ReLU}(X + R)$.

Additionally, some games are played with a *komi* (compensation given to White for playing second) that is not equal to the value of 7.5 used by Silver et al. (2017). Therefore, for the final feature of the input encoding, rather than a binary-valued feature equalling 1 if the player to move is White and 0 if the player to move is Black, we instead use the real-valued feature of $\text{komi}/10$ if the player to move is White or $-\text{komi}/10$ if the player to move is Black. We additionally exclude a very tiny number of games with extreme komi values, outside of the range $[-60, 60]$.

We train using a mini-batch size of 2048 distributed as 8 batches of 256 across 8 GPUs, and train for a total of 64 epochs - roughly 475000 minibatches for the GoGoD dataset. We use SGD with momentum 0.9, weight decay coefficient of $1e-4$, and a learning rate schedule of $1e-1$, $1e-2$, $1e-3$, $1e-4$ for the first 16, next 16, next 16, and last 16 epochs respectively.

We train both the policy and values heads jointly, minimizing the cross entropy of the policy head with respect to the one-hot move made in the actual game, and the MSE of the value head with respect to the game result of -1 or 1, except similarly to Silver et al. (2017) we weight the MSE value loss by 0.01 to avoid overfitting of the value head.

I. MCTS Algorithmic Details

Recall that in MCTS, similar to that of Silver et al. (2017), we descend the tree by choosing actions according to:

$$\arg \max_a Q(s, a) + c_{\text{puct}} \tau(s, a) \frac{\sqrt{\sum_b N(s, b)}}{N(s, a) + 1}$$

where $Q(s, a)$ is the average future reward estimate returned from all times where action a was explored from state s in the search so far from the perspective of the player whose turn it is at state s . For our work, we follow the convention where win, loss, and draw have reward 1, -1, and 0.

Since the tree policy depends on the $Q(s, a)$ estimates of the possible actions, there is a nontrivial choice of what Q value to use for an action a that has been tried *zero* times and therefore never estimated. Since the tree branches exponentially, deeper in the MCTS tree there will always be many actions with zero visits, and so this choice can affect the behavior of MCTS even in the limit of large amounts of search. Unfortunately, the details of this choice have sometimes been left undiscussed and undocumented in major past work, and as a result major MCTS implementations have not standardized on it, variously choosing game-loss (Lai, 2018), the current running average parent Q or a Q -value minus a heuristic offset parameter (Tian, 2019), or many other options. In our work, we use the equal-weighted average value of all actions at the parent node that have been visited at least once, i.e. $\sum_a Q(s, a) I(N(s, a) > 0) / \sum_a I(N(s, a) > 0)$. This can be viewed as corresponding to a naive prior that the values of actions are i.i.d draws from an unknown distribution. While not necessarily optimal, our choice is simple, parameter-free, behaves in a way that is invariant to any global translation or scaling of the game’s rewards, and works reasonably in practice for our purposes.